CJC Pediatric and Congenital Heart Disease 1 (2022) 136–157

Review

Echocardiographic Assessment of Right Ventricular Function in Paediatric Heart Disease: A Practical Clinical Approach

Kandice Mah, MD,[a] and Luc Mertens, MD[b]

[a] Division of Cardiology, BC Children's Hospital, University of British Columbia, Vancouver, British Columbia, Canada

[b] Department of Paediatrics, Labatt Family Heart Centre, the Hospital for Sick Children, University of Toronto, Toronto, Ontario, Canada

ABSTRACT

As the right ventricle (RV) plays an integral role in different paediatric heart diseases, the accurate assessment of RV size and function is essential in the diagnosis, management, and prognostication of congenital and acquired cardiac lesions. Yet, echocardiographic evaluation of the RV is challenging because of its complex and variable morphology, its different physiology compared with the left ventricle, and its capability to adapt to different loading conditions associated with congenital and acquired heart diseases within certain ranges. Reliable echocardiographic detection of RV systolic and diastolic dysfunction remains challenging while important for patient management. This review provides an updated, practical approach to assessing RV function in structurally normal hearts and in children with common congenital heart defects and in those with pulmonary hypertension. We also review the impact of tricuspid valve function on RV functional parameters. There is no single functional RV parameter that

RÉSUMÉ

Étant donné que le ventricule droit (VD) joue un rôle déterminant dans diverses cardiopathies pédiatriques, l'évaluation précise de sa taille et de sa fonction s'avère essentielle pour le diagnostic, la prise en charge et le pronostic des lésions cardiaques congénitales et acquises. Pourtant, il s'avère difficile d'effectuer une évaluation échocardiographique du VD en raison de sa morphologie complexe et variable, des caractéristiques physiologiques qui le distingue du ventricule gauche et de sa capacité à s'adapter dans une certaine mesure à différentes conditions de charge associées aux cardiopathies congénitales et acquises. La détection échocardiographique fiable des dysfonctions systolique et diastolique du VD représente encore un défi, tout en étant importante pour la prise en charge des patients. Le présent article de synthèse propose une approche pratique et actualisée pour l'évaluation de la fonction ventriculaire droite en l'absence d'anomalie structurelle cardiaque, de même qu'en présence

The assessment of right ventricular (RV) function is essential in the diagnosis and management of different paediatric cardiac lesions, including congenital heart disease (CHD) and pulmonary hypertension (PH). Indices of RV size and function are prognostic in a wide range of congenital and paediatric cardiac diseases.[1,2] Although cardiac magnetic resonance imaging (MRI) is often considered the clinical reference technique for RV functional assessment, its more limited availability, need for sedation or anaesthesia in younger children, and its cost are obvious limitations for regular clinical use. Echocardiography remains the first-line clinical technique in the routine follow-up of different paediatric cardiac conditions affecting the RV. Echocardiographically, the RV can be assessed qualitatively and quantitatively with routine 2D imaging as well as with more advanced echocardiographic techniques. Complete echocardiographic evaluation includes the assessment of right atrial size, RV size, RV systolic function, RV systolic pressure, and RV diastolic function.[3,4]

The echocardiographic assessment of RV function in paediatric heart disease is challenging because of the wide variability in both morphology and physiology. Although normal reference data for right heart size and function in paediatrics are available, their use in the different pathologic conditions is more challenging. For instance, what is considered as "normal" RV function in a systemic RV or hypoplastic left heart syndrome (HLHS) may differ significantly from what is considered normal for a patient with an atrial septal defect (ASD) or after tetralogy of Fallot (TOF) repair. The practical utility of some of the reference data is further affected by changes with age and body size. This leads to the additional consideration of factoring in what normal is between different age groups as well as between different disease conditions. Interpreting RV dimensions and functional parameters requires understanding the different disease states, as will be discussed below.

Received for publication April 2, 2022. Accepted May 5, 2022.

Corresponding author: Dr Kandice Mah, Division of Cardiology, BC Children's Hospital, 4480 Oak St, Vancouver, British Columbia V6H 3N1, Canada. Tel.: +1-604-875-2296; fax: 604-875-2774.

E-mail: kandice.mah@cw.bc.ca

https://doi.org/10.1016/j.cjcpc.2022.05.002

uniquely describes RV function; instead a combination of different parameters is recommended in clinical practice. Qualitative and quantitative analysis of RV function will be reviewed including more recent techniques such as speckle tracking and 3D echocardiography.

d'anomalies cardiaques congénitales courantes ou d'hypertension pulmonaire chez les enfants. Nous examinons également l'effet de la fonction valvulaire tricuspide sur les paramètres de la fonction ventriculaire droite. Aucun paramètre fonctionnel pris isolément ne suffit à décrire la fonction ventriculaire droite; le recours à une combinaison de différents paramètres est plutôt recommandé en pratique clinique. L'analyse qualitative et quantitative de la fonction ventriculaire droite sera abordée, y compris des techniques plus récentes telles que l'échocardiographie de suivi des marqueurs acoustiques (*speckle tracking*) et l'échocardiographie tridimensionnelle.

As for any other echocardiographic technique, it is essential to standardize quantitative methods to be able to track changes over time based on serial measurements. This allows us to identify how RV function evolves in different pathologies. Serial trends in quantitative measures are prognostically important in different conditions.

In this review, we will discuss the echocardiographic assessment of a normal RV and in different cardiac disorders associated with increased RV pressure and volume loading. This paper aims to provide a practical guide on how to use echocardiography in clinical practice to monitor RV function in children.

Normal RV Anatomy and Architecture

The RV is a crescent-shaped and thin-walled structure with 10%-15% of the volume and one-sixth to one-third less mass than the left ventricle (LV).[5,6] The RV has 3 components: the inlet (which includes the tricuspid valve [TV], tendinous chords, and 3 or more papillary muscles), the trabeculated and very thin-walled apex, and the muscular trabecular outlet/infundibulum.[7]

A normal RV has 2 layers composed of (1) circumferential superficial myocytes that make up 25% of the RV wall and (2) longitudinal subendocardial myocytes that pass through the apex towards the papillary muscles, tricuspid annulus, and RV outflow.[7] This configuration is optimally designed to support a low-pressure high-compliance pulmonary circulation. This differs from the LV that has 3 myocardial layers with a progressive transition from (1) subepicardial left-handed spiralling with more longitudinally oriented fibres to (2) a thick middle layer with more circumferentially oriented fibres to (3) subendocardial right-handed spiralling with more longitudinally oriented fibres.[8] This fibre organization results in a predominant contribution of circumferential shortening for LV function, whereas for the normal RV, longitudinal shortening is the dominant motion contributing to RV output.[4] The opposite spiralling from epicardium to endocardium results in a counterclockwise motion of the LV apex relative to the LV base that results in twisting of the LV during systole and untwisting during diastole.[8] This wringing motion is not present in the normal RV.[7,9] Instead the deep trabeculations in the RV apex serve as a sponge that is an important contributor to systolic RV output.[9] The ventricles also have a functional interdependence with epicardial RV and LV fibres that extend from one ventricle to the other, and shared longitudinal RV myocytes that are continuous with septal fibres and the pericardial space.[7,9,10]

Normal TV Anatomy and Architecture

The TV usually has 3 leaflets (anterior, septal, and posterior) with large variability in leaflet morphology. Clefts and additional scallops are common even in normally functioning TVs.[11] The anterior leaflet usually is the largest and the most mobile, whereas the septal and posterior leaflets vary more in size and mobility.[11] The septal leaflet chords insert into a septal papillary muscle that makes septal leaflet function and position sensitive to ventricular septal shifts that can occur in RV pressure and volume loading.[11]

The TV annulus is an asymmetrical, saddle-shaped ellipsoid that is narrower in the septal-lateral direction than the anterior-posterior direction, with a higher anterior-posterior peak and lower lateral-septal peak.[12,13] Through the cardiac cycle, the annulus changes its shape and size. In early diastole, as the ventricle fills, the TV annulus dilates and is at its maximal bending angle.[12] In early systole, the annular area decreases by 16% and the annulus flattens.[13] This allows for optimal leaflet coaptation and minimizes the stress on the valve. Normal valves have some prolapse and tethering of the leaflets and a 90° angle of the papillary muscle to the annular plane that distributes the annular-leaflet-chordal stress in a nondilated heart.[13,14] The presence of the LV is fundamental for TV shape and function as it provides a lateral force that causes contraction of the free wall towards the septal wall (bellowing of the RV).[13] This maintains the elliptical shape of the TV annulus and allows the septal leaflet to act as a door jamb for the anterior and posterior leaflets to adequately coapt against.[13] This explains the close interaction between TV function and RV size, shape, and ventricular function.

Echocardiographic Assessment of the Normal RV

The assessment of the normal RV includes the assessment of RV chamber dimensions, RV systolic function, and RV diastolic function.

Right heart dimensions

Measuring dimensions of RV structures has been included in adult guidelines for performing echocardiograms.[3,4] Also for paediatric echocardiographic studies, recommendations of how to quantify right heart dimensions have been published, including measurements of the right atrium (RA), RV, TV annulus, pulmonary valve annulus, and branch pulmonary arteries (PA).[15] Figure 1 illustrates RV 2-dimensional measurements that can be obtained from the RV-centric apical 4-chamber view. From apical views, it can be difficult to avoid

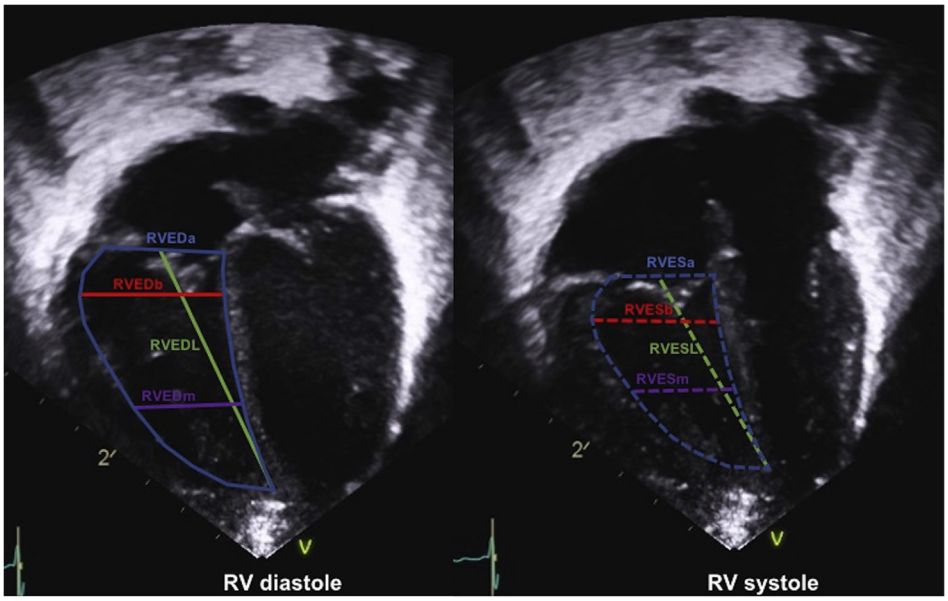

Figure 1. Right ventricular (RV) measurements in systole and diastole.[23,24] Standardized measurement locations of the RV in the RV-centric 4-chamber view. RVEDa, right ventricular end-diastolic mid-ventricular area; RVEDb, right ventricular end-diastolic basal width; RVEDL, right ventricular end-diastolic length; RVEDm, right ventricular end-diastolic mid-ventricular width; RVESa, right ventricular end-systolic mid-ventricular area; RVESb, right ventricular end-systolic basal width; RVESL, right ventricular end-systolic length; RVESm, right ventricular end-systolic mid-ventricular width.

RV foreshortening, and even slight rotation of the probe can result in different RV size measurements.[16] Therefore, consistent standardization is essential if measurements are used for decision-making in pathology. Two-dimensional echocardiographic measurements typically underestimate RV dimension when compared with MRI-based measurements.[17] From all the different dimensions used, RV end-diastolic area best correlates with MRI RV end-diastolic volumes, and indexed RV end-diastolic areas can be used in the serial follow-up of patients as a substitute for RV volumetric MRI measurements.[17]

Using quantitative measurements in paediatrics can be more difficult than in the adult population because of the changes in body size, as children are growing at variable rates. This typically makes it difficult to define normal values. The accuracy of generated "normal data" can be further limited by the number of healthy subjects included, lack of standardization, different methods used for normalization of body size measurements, and variations in how the values are presented.[18] Lack of standardization can affect the precision in estimating the severity of defects, especially in neonates, and can bias clinical decision-making.[18,19] Despite these limitations, *z*-scores are considered to be the best method to normalize echocardiographic measurements in children. Yet there are few studies specifically trying to establish RV-specific *z*-scores.

The most used *z*-scores systems in North America are the Boston *z*-scores (https://zscore.chboston.org)[20] and more recently the Pediatric Heart Network *z*-scores (http://www.parameterz.com/refs/lopez-circimaging-2017).[21] The last are based on a multicentre effort including measurements from normal echocardiograms in 3566 North American children.[21] It includes measurements of the TV annulus, pulmonary valve annulus, main PA, and proximal PA branches. It does not however include measurements of RV dimensions.[21] Recently the 2 most commonly used *z*-score systems were compared with few differences noted.[22] The same *z*-score model should however be used for practice guidelines and medical decision-making at each institution.[22] When published *z*-scores are used, it is also important to look at how the measurements were obtained, as the technique may influence the measurements that are made.

A more comprehensive list of specific normal paediatric RV measurements was published by Koestenberger[23] and Wang[24] (Table 1). All larger studies used the Haycock formula for body surface area (BSA), but they observed a residual variation in the results after correcting for BSA, indicating that correcting for BSA alone may not be the best method of normalization for paediatric data.[25] Also, when height was used for standardization, variability persisted.[23,24]

Practical approach to assessing RV size

Practical measures to track RV size over time are TV annulus size and RV end-diastolic area indexed for BSA. The last measure has the advantage of not requiring *z*-scores and has been demonstrated to correlate well with RV volumes by MRI.[17]

Right ventricular systolic function

Although for LV function, LV ejection fraction (EF) has been well established as a clinical reference method for assessing LV pump function, it is more difficult to obtain RV EF related to the more complex RV geometry and its anterior

Table 1. Normal RV dimensions[23,24]

BSA (m^2)	RVOTd (cm)	RVOTs (cm)	RVEDb (cm)	RVESb (cm)	RA length (cm)	Length (cm)	RVEDL (cm)	RVESL (cm)	RVEDb (basal RV, cm)	RVEDm (mid-RV, cm)	RVEDa (cm^2)	RVESa (cm^2)
0.1[24]	0.53 (0.19-0.88)	0.28 (0.00-0.61)	0.91 (0.36-1.46)	0.91 (0.38-1.44)	1.00 (0.62-1.38)	50[23]	2.3 (1.3-3.3)	1.7 (1.2-2.3)	1.3 (0.7-1.9)	1.2 (0.6-1.7)	2.5 (1.5-4.0)	1.4 (0.8-2.4)
0.15[24]	0.62 (0.28-0.97)	0.39 (0.05-0.72)	1.06 (0.51-1.61)	1.00 (0.47-1.53)	1.15 (0.77-1.53)	55[23]	2.5 (1.5-3.5)	1.8 (1.3-2.4)	1.4 (0.8-2.0)	1.2 (0.7-1.8)	2.9 (1.8-4.7)	1.6 (1.0-2.8)
0.2[24]	0.71 (0.37-1.06)	0.49 (0.16-0.82)	1.20 (0.65-1.75)	1.09 (0.56-1.62)	1.29 (0.91-1.67)	60[23]	2.6 (1.6-3.7)	1.9 (1.4-2.6)	1.5 (0.9-2.1)	1.3 (0.7-1.9)	3.3 (2.1-5.4)	1.9 (1.1-3.2)
0.25[24]	0.80 (0.45-1.14)	0.58 (0.25-0.92)	1.33 (0.78-1.88)	1.17 (0.64-1.70)	1.43 (1.05-1.80)	65[23]	2.8 (1.8-3.9)	2.0 (1.5-2.7)	1.6 (1.0-2.2)	1.4 (0.8-2.0)	3.8 (2.4-6.1)	2.2 (1.3-3.6)
0.3[24]	0.87 (0.53-1.22)	0.67 (0.34-1.01)	1.45 (0.90-2.00)	1.25 (0.72-1.78)	1.55 (1.17-1.93)	70[23]	3.0 (1.9-4.0)	2.1 (1.6-2.9)	1.7 (1.0-2.3)	1.5 (0.9-2.1)	4.3 (2.7-6.8)	2.4 (1.5-4.1)
0.35[24]	0.95 (0.60-1.29)	0.76 (0.42-1.09)	1.56 (1.01-2.11)	1.33 (0.80-1.86)	1.66 (1.29-2.04)	75[23]	3.2 (2.1-4.2)	2.2 (1.7-3.0)	1.8 (1.1-2.4)	1.6 (1.0-2.2)	4.8 (3.0-7.6)	2.7 (1.6-4.6)
0.4[24]	1.02 (0.67-1.36)	0.84 (0.50-1.17)	1.67 (1.12-2.22)	1.40 (0.87-1.93)	1.77 (1.39-2.15)	80[23]	3.3 (2.3-4.4)	2.4 (1.7-3.2)	1.9 (1.2-2.5)	1.7 (1.0-2.3)	5.3 (3.4-8.4)	3.1 (1.8-5.1)
0.45[24]	1.08 (0.74-1.43)	0.91 (0.58-1.24)	1.77 (1.22-2.32)	1.47 (0.94-2.00)	1.87 (1.49-2.25)	85[23]	3.5 (2.4-4.6)	2.5 (1.8-3.3)	2.0 (1.3-2.6)	1.7 (1.1-2.4)	5.9 (3.7-9.2)	3.4 (2.0-5.6)
0.5[24]	1.14 (0.80-1.49)	0.98 (0.64-1.31)	1.86 (1.31-2.41)	1.54(1.01-2.07)	1.97 (1.59-2.34)	90[23]	3.7 (2.6-4.8)	2.6 (1.9-3.5)	2.1 (1.4-2.8)	1.8 (1.2-2.5)	6.4 (4.1-10.1)	3.7 (2.2-6.1)
0.6[24]	1.25 (0.91-1.60)	1.10 (0.76-1.43)	2.02 (1.47-2.57)	1.66 (1.13-2.19)	2.13 (1.75-2.51)	95[23]	3.9 (2.8-5.0)	2.7 (2.0-3.7)	2.1 (1.4-2.9)	1.9 (1.2-2.5)	7.0 (4.5-11.0)	4.1 (2.5-6.7)
0.7[24]	1.35 (1.00-1.69)	1.20 (0.87-1.53)	2.16 (1.61-2.71)	1.78 (1.24-2.31)	2.27 (1.89-2.65)	100[23]	4.0 (2.9-5.2)	2.8 (2.1-3.8)	2.2 (1.5-3.0)	2.0 (1.3-2.6)	7.7 (4.9-11.9)	4.4 (2.7-7.3)
0.8[24]	1.43 (1.08-1.77)	1.29 (0.95-1.62)	2.28 (1.72-2.83)	1.88 (1.35-2.41)	2.39 (2.01-2.77)	105[23]	4.2 (3.1-5.4)	3.0 (2.2-4.0)	2.3 (1.6-3.1)	2.1 (1.4-2.7)	8.3 (5.4-12.8)	4.8 (2.9-7.9)
0.9[24]	1.50 (1.15-1.85)	1.36 (1.02-1.69)	2.38 (1.82-2.93)	1.97 (1.44-2.50)	2.48 (2.10-2.86)	110[23]	4.4 (3.3-5.5)	3.1 (2.3-4.2)	2.4 (1.7-3.2)	2.1 (1.5-2.8)	8.9 (5.8-13.8)	5.2 (3.2-8.5)
1[24]	1.56 (1.21-1.91)	1.41 (1.08-1.75)	2.46 (1.91-3.01)	2.06 (1.53-2.59)	2.56 (2.18-2.94)	115[23]	4.6 (3.4-5.7)	3.2 (2.4-4.4)	2.5 (1.7-3.3)	2.2 (1.5-2.9)	9.6 (6.3-14.8)	5.6 (3.4-9.1)
1.1[24]	1.61 (1.27-1.96)	1.46 (1.13-1.79)	2.53 (1.98-3.08)	2.13 (1.60-2.67)	2.62 (2.25-3.00)	120[23]	4.8 (3.6-5.9)	3.4 (2.5-4.5)	2.6 (1.8-3.4)	2.3 (1.6-3.0)	10.3 (6.7-15.8)	6.0 (3.7-9.8)
1.2[24]	1.65(1.31-2.00)	1.49 (1.16-1.83)	2.59 (2.04-3.14)	2.20 (1.67-2.74)	2.67 (2.30-3.05)	125[23]	4.9 (3.7-6.1)	3.5 (2.6-4.7)	2.7 (1.9-3.5)	2.4 (1.7-3.1)	11.0 (7.2-16.8)	6.4 (3.9-10.4)
1.3[20]	1.69 (1.35-2.04)	1.52 (1.19-1.85)	2.64 (2.09-3.19)	2.27 (1.74-2.80)	2.71 (2.33-3.09)	130[19]	5.1 (3.9-6.3)	3.7 (2.7-4.9)	2.8 (2.0-3.6)	2.5 (1.8-3.2)	11.7 (7.7-17.9)	6.8 (4.2-11.1)
1.4[20]	1.72 (1.38-2.07)	1.54 (1.21-1.87)	2.69 (2.13-3.24)	2.32 (1.79-2.86)	2.74 (2.36-3.12)	140[19]	5.5 (4.2-6.7)	4.0 (3.0-5.3)	3.0 (2.2-3.8)	2.6 (1.9-3.4)	13.3 (8.8-20.1)	7.7 (4.8-12.5)
1.5[20]	1.75 (1.41-2.10)	1.55 (1.22-1.89)	2.73 (2.18-3.28)	2.38 (1.85-2.91_	2.77 (2.39-3.15)	150[19]	5.8 (4.6-7.0)	4.3 (3.2-5.7)	3.1 (2.3-4.0)	2.8 (2.0-3.5)	14.8 (9.8-22.3)	8.7 (5.4-14.0)
1.6[20]	1.78 (1.44-2.13)	1.56 (1.23-1.89)	2.77 (2.22-3.33)	2.43 (1.89-2.96)	2.79 (2.41-3.17)	160[19]	6.2 (4.9-7.4)	4.6 (3.5-6.1)	3.3 (2.5-4.2)	3.0 (2.2-3.7)	16.5 (11.0-24.7)	9.7 (60-15.5)
1.7[20]	1.81 (1.46-2.15)	1.57 (1.24-1.90)	2.82 (2.27-3.37)	2.47 (1.94-3.00)	2.81 (2.43-3.19)	170[19]	6.5 (5.2-7.8)	4.9 (3.7-6.5)	3.5 (2.6-4.4)	3.1 (2.3-3.9)	18.2 (12.2-27.1)	10.7 (6.7-17.1)

RVOTd: Parasternal long axis, m-mode echocardiographic measurement at end diastole
RVOTs: Parasternal long axis, m-mode echocardiographic measurement at end systole
RVEDb: Apical 4-chamber, distance between the RV free wall and septum at end diastole, distal to the TV annulus
RVESb: Apical 4-chamber, distance between the RV free wall and septum at end systole, distal to the TV annulus
RA: Apical 4-chamber, max left to right dimensions during systole

RVEDL: Apical 4-chamber, RV mid-cavity length at end diastole, from the midpoint of the TV annulus to apex
RVESL: Apical 4-chamber, RV mid-cavity length at end systole, from the midpoint of the TV annulus to apex
RVEDb: Apical 4-chamber, distance between the RV free wall and septum at end diastole, distal to the TV annulus
RVEDm: Apical 4-chamber, distance between the RV free wall and septum at end diastole, mid-third of RV at the level of the LV papillary muscle
RVEDa: Apical 4-chamber, RV end-diastolic area
RVESa: Apical 4-chamber, RV end-systolic area

Values: mean (±2 SD range).

BSA, body surface area; RA, right atrium; RV, right ventricle; RVED, right ventricular end diastolic; RVEDa, right ventricular end-diastolic mid-ventricular area; RVEDb, right ventricular end-diastolic basal width; RVEDL, right ventricular end-diastolic length; RVEDm, right ventricular end-diastolic mid-ventricular width; RVES, right ventricular end systolic; RVESa, right ventricular end-systolic mid-ventricular area; RVESb, right ventricular end-systolic basal width; RVESL, right ventricular end-systolic length; RVOT, right ventricular outflow tract; RVOTd, RV outflow tract (diastole); RVOTs, RV outflow tract (systole).

Parameter	Image	Normal parameters	Advantages	Limitations
RVFAC[4]	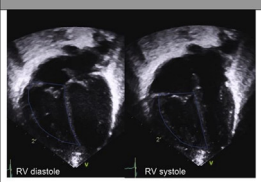 $\text{RVFAC} = \frac{\text{RV end diastolic area} - \text{RV end systolic area}}{\text{RV end diastolic area}}$	>35%	• Reproducible • Simple to use • Correlates with RV EF	• Geometry and window dependent • Does not include RV outflow • Load dependent
TAPSE[35]	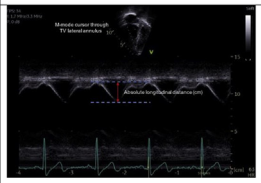	Normal: Table 2 Dysfunction < lower-limit	• Window independent • Reproducible • Simple to use • Correlates with RVFAC and RV EF if no regional dysfunction	• Angle Dependent • Regional assessment • Load dependent • Influenced by valve regurgitation
Tricuspid annular S'[40,41]	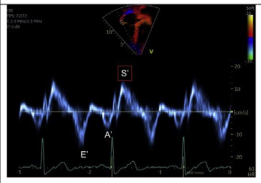	Normal: Fig 3 Dysfunction < lower-limit	• Reproducible • Simple to use	• Angle dependent • Load dependent • Age (cardiac mass) dependent • HR correction if >100 or <70 bpm
RV MPI (aka RIMP, Tei Index)[4,47]	**Tissue Doppler Method:** 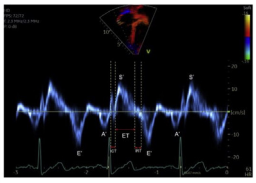 $\text{Tei Index} = \frac{\text{ICT} + \text{IRT}}{\text{ET}} = \frac{a - b}{b}$	Reflects loading more than contractility Post-op TOF: MPI >0.40 correlated with CMR RVEF <35%	• Useful in PHTN and TOF	• Limited RV utility (very short isovolumic periods) • Load dependent • Requires regular HR • PW method not possible in RV
RV longitudinal Strain[57,62,153]	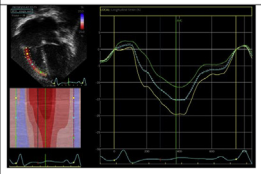	Normal: Table 3 Dysfunction <15%	• Geometry independent • Detects regional changes • Angle independent • Regional or global assessment	• Poor reproducibility • Reference values limited • High frame rates • Load dependent • Normal RV: longitudinal strain only

RVFAC: RV fractional area change, RV: Right ventricle, EF: Ejection Fraction, RAp: Right atrial pressure, TR: Tricuspid Regurgitation, ICT: Isovolumic contraction time, IRT: Isovolumic relaxation time, ET: Ejection time, TDI: Tissue Doppler Imaging, TAPSE: Tricuspid annular plane systolic excursion

Figure 2. Overview of methods for RV systolic function. CMR, cardiac MRI; HR, heart rate; MPI, myocardial performance index; PHTN, pulmonary hypertension; PW, pulse-wave; TOF, tetralogy of Fallot; TV, tricuspid valve.

position in the chest. Although 3D-based RV EF has been available for a while and has been proven to correlate well with MRI-based RV EF,[26] its utility in daily paediatric practice is still quite low, mainly related to the difficulty in obtaining good RV 3D volumes, especially in dilated hearts. This results in difficulties identifying endocardial borders of all the walls. Also, the 3D RV EF programs are still relatively time-consuming, especially when compared with the more automated LV EF calculations. Some laboratories have introduced 3D RV EF for specific patient groups known to be at high risk for developing RV dysfunction including patients after TOF repair[27] and those with PH.[28] As this is not feasible for a larger group of patients,[29] several easier 2D-based measurements have been proposed for routine clinical practice. Each of these parameters has specific limitations for the assessment of RV systolic function, as such a combination of different parameters should be used in patient follow-up.

RV fractional area change—2D. As RV areas have been demonstrated to reflect RV volumes relatively well, the change in RV area from end diastole to end systole can be used as a substitute for volumetric RV EF.[15–17] RV fractional area change (RVFAC) is obtained from the apical 4-chamber or RV-centric views and correlates well with RV EF when RV dysfunction is global with no significant regional differences, particularly involving the RV outflow tract.[16] RVFAC represents inlet and apical function and does not include the RV outlet (Fig. 2). In patients with regional outflow tract dysfunction such as patients after TOF repair, RVFAC can overestimate RV EF calculated by MRI.[30] Two-dimensional FAC of <35% indicates RV systolic dysfunction.[31] One of the limitations of this method is that visualization of the entire RV free wall endocardial border from the annulus to apex both in systole and diastole can be difficult. Image optimization during the acquisition is required, but lung interposition can interfere with image quality. Interobserver variability can be high and the tracing must be well standardized with the inclusion of the RV trabeculations in the area calculation as this reduces variability.[4,16] Like RV EF, FAC is influenced by loading conditions; it needs to be interpreted cautiously in case of acute alterations in loading.

Tricuspid annular plane systolic excursion. Tricuspid annular plane systolic excursion (TAPSE) is measured by M-mode at the TV free wall annulus. It reflects longitudinal systolic displacement of the lateral TV annulus during systole (Fig. 2).[4] As such, it is a regional parameter, and, when used as a global RV functional parameter, it assumes that annular displacement represents global RV function.[4] It is also influenced by different factors such as tricuspid regurgitation (TR) (increased preload), ventricular interactions (basal RV function can be passively pulled by the LV in the case of RV dysfunction), and RV dyssynchrony (apical rocking will result in basal displacement changes).[32] In adult recommendations, TAPSE >1.7 cm is considered normal but the relationship between TAPSE and RV EF is variable as TAPSE is influenced by different confounders.[4] Also in the progression of RV dysfunction, the RV apex can be involved first with relative preservation of basal RV function.[33] Thus, when using TAPSE as the only RV functional parameter, earlier stages of RV dysfunction may be missed. Changes in TAPSE can occur in later stages of RV dysfunction, and this likely explains why decreased TAPSE a strong predictor of adverse outcomes in different diseases affecting the RV, such as PH.[34]

Table 2. TAPSE by age and BSA

Age	BSA (m^2)	TAPSE (cm)
0-30 d	0.23 (0.17-0.28)[36]	1.06 (0.66-1.45)[36]
	0.22 (0.14-0.28)[35]	0.91 (0.68-1.15)[35]
		0.91 (0.64-1.18)[153]
1-3 mo	0.28 (0.21-0.44)[36]	1.30 (0.93-1.66)[36]
	0.29 (0.12-0.54)[35]	1.14 (0.85-1.42)[35]
		1.05 (0.71-1.39)[153]
4-6 mo	0.34 (0.29-0.56)[36]	1.42 (1.01-1.83)[36]
	0.34 (0.26-0.41)[35]	1.31 (1.01-1.65)[35]
		1.19 (0.83-1.56)[153]
7-12 mo	0.41 (0.29-0.56)[36]	1.52 (0.91-2.12)[36]
	0.40 (0.31-0.47)[35]	1.44 (1.13-1.77)[35]
		1.35 (0.77-1.92)[153]
1-2 y	0.54 (0.27-0.75)[36]	1.71 (1.13-2.29)[36]
		1.57 (1.06-2.09)[153]
1 y	0.47 (0.3-0.69)[35]	1.55 (1.25-1.88)[35]
2 y	0.53 (0.4-0.62)[35]	1.65 (1.36-1.94)[35]
3-4 y	0.72 (0.32-1.07)[36]	1.94 (1.41-2.46)[36]
		1.81 (1.33-2.29)[153]
3 y	0.63 (0.52-0.77)[35]	1.74 (1.48-2.02)[35]
4 y	0.70 (0.60-0.91)[35]	1.82 (1.56-2.07)[35]
5-8 y	0.93 (0.52-1.35)[36]	1.93 (1.36-2.51)[36]
		2.01 (1.45-2.57)[3]
5 y	0.77 (0.63-0.99)[35]	1.87 (1.60-2.13)[35]
6 y	0.82 (0.46-1.06)[35]	1.90 (1.62-2.18)[35]
7 y	0.94 (0.75-1.17)[35]	1.94 (1.64-2.25)[35]
8 y	0.97 (0.79-1.39)[35]	1.97 (1.67-2.28)[35]
9-12 y	1.28 (0.46-1.7)[36]	2.10 (1.47-2.73)[36]
		2.30 (1.63-2.96)[153]
9 y	1.00 (0.8-1.32)[35]	2.01 (1.73-2.30)[35]
10 y	1.15 (0.82-1.54)[35]	2.05 (1.79-2.31)[35]
11 y	1.28 (1.06-1.55)[35]	2.10 (1.83-2.36)[35]
12 y	1.39 (1.08-1.67)[35]	2.14 (1.84-2.43)[35]
13-18 y	1.59 (1.33-2.04)[36]	2.10 (1.44-2.75)[36]
		2.59 (1.87-3.31)[153]
13 y	1.48 (1.03-1.87)[35]	2.20 (1.85-2.54)[35]
14 y	1.55 (1.11-1.93)[35]	2.26 (1.86-2.65)[35]
15 y	1.59 (1.32-1.96)[35]	2.33 (1.93-2.75)[35]
16 y	1.66 (1.3-2.04)[35]	2.39 (1.98-2.78)[35]
17 y	1.77 (1.43-2.06)[35]	2.45 (2.04-2.88)[35]
18 y	1.79 (1.34-2.25)[35]	2.47 (2.05-2.91)[35]

TAPSE: mean (2SD); BSA: mean (min-max range).

BSA, body surface area; TAPSE, tricuspid annular plane systolic excursion.

Application of TAPSE in paediatric echocardiography is complicated by the fact that TAPSE measurements are influenced by cardiac size and thus by growth and body size. This influences the routine application of TAPSE in paediatric patients as changes may be related to growth. Koestenberger et al. established normal values for different ages and BSA (Table 2).[35,36] An additional confounding factor in patients with CHD is that TAPSE decreases postoperatively despite normal RV systolic function, which is likely related to adhesions between the surrounding tissue at the basal RV that can impact longitudinal motion of the RV annulus and base.[37,38] A decrease in TAPSE in postoperative patients thus does not necessarily reflect RV dysfunction.[38] For certain paediatric patients, tracking TAPSE over time can however be useful as a progressive decrease in TAPSE is typically not expected as children grow.[38,39] As TAPSE is a relatively easy and

reproducible measurement, it should be included in the serial follow-up of patients at risk of developing RV dysfunction.

RV systolic tissue Doppler velocity (S′). Tissue Doppler imaging (TDI) from the 4-chamber view RV free wall of the TV annular or basal RV myocardial velocity is a measure of the longitudinal displacement velocity (Fig. 2). It thus represents the speed at which the annulus moves during systole, and the peak systolic velocity (S′) measurement is an index for RV longitudinal systolic function.[4] As a Doppler measurement, it is angle dependent and requires good alignment of the ultrasound beam with the direction of motion, which can be challenging in more dilated hearts.[40,41] Care should be taken to avoid overgaining the Doppler envelope, which can result in overestimation. The measurement of S′ is easy and reproducible, but by definition this is a regional measurement that correlates weakly with measurements of global RV systolic function.[42] The septal TDI velocity represents both RV and LV longitudinal function and as such should not be used to assess RV function.[4] In adults, a normal TV S′ is >9.5 cm/s and has been shown to discriminate between normal and abnormal RV EF.[4] It is influenced not only by myocardial function but also by translational cardiac motion, tethering, dyssynchrony, ventricular interactions, and loading conditions.[43] In paediatrics, normal S′ values are age and heart rate dependent, which again limits its use in clinical practice as a method for assessing systolic function (Fig. 3).[40,44,45] As it is simple and reproducible, it has been used to assess RV function in CHD,[46] but with the introduction of RV strain measurements, the clinical utility of S′ has decreased.

RV myocardial performance index. RV myocardial performance index (MPI, also known as the Tei index) is considered a combined measure of RV systolic and diastolic function as it combines isovolumetric contraction and relaxation time intervals, corrected for ejection time.[4] MPI is defined as the ratio of isovolumic time intervals divided by ejection time, or [(IRT + ICT)/ET] (Fig. 2).[4] It is applicable for a broad range of heart rates but requires a regular R-R interval.[4] MPI can be obtained by 2 methods: pulse wave Doppler and TDI. When using pulse wave Doppler, for the RV it requires acquiring simultaneous inflow (beginning of the tricuspid inflow E wave to end of the tricuspid inflow A wave) and outflow (onset to the cessation of flow) Doppler traces to determine isovolumic time and ejection time. The problem with MPI for the RV is that it is influenced by respiration and it is nearly impossible to obtain inflow and outflow simultaneously, making the pulse wave Doppler method for MPI acquisition more difficult. The TDI method has the advantage of requiring 1 trace only (TV annulus). The TDI method is standardized by BSA as it is impacted by heart size.[47] Values higher than the upper limit are considered to be abnormal. In adults, MPI has prognostic value in cardiomyopathy and PH at a single time point and correlates with clinical change.[4] In paediatrics, it has the theoretical advantage of being geometry independent that is useful in the CHD[47,48] and PH populations.[49] The disadvantage is that the index is load sensitive.[50] For instance, MPI paradoxically improves when filling pressures increase, as this shortens the isovolumetric relaxation time.[50] Another problem is that it combines systolic and diastolic dysfunction and thus only indicates that "something" is wrong with RV function without identifying what is wrong. Finally, as for any timing parameter, the reproducibility is poor, which further limits its use in clinical practice. It has largely been abandoned in most clinical laboratories as the utility is limited and other methods provide better information.

RV longitudinal strain and strain rate. Speckle tracking echocardiography (STE) allows the assessment of myocardial function by measuring the myocardial deformation that occurs during the cardiac cycle.[4] An object or medium under stress becomes deformed and strain represents percentage change of deformation when stress is applied. As such, it is a dimensionless number. Strain is the result of the net stress on the myocardium that is determined by a combination of contractility and loading and is influenced by tissue elasticity. Thus, by definition, strain is influenced by loading conditions.[51,52] Myocardial deformation is multidimensional but for simplicity is typically assessed using a Cartesian system based on standard 2D views. For the LV, from apical 4-, 2-, and 3-chamber views, longitudinal strain can be assessed. From the short axis views, circumferential and radial strain can be measured.[4] In longitudinal and circumferential strain, shortening occurs in systole and lengthening in diastole. In radial strain, thickening is in systole and thinning is in diastole. Strain rate represents the rate of deformation over time, and peak systolic strain rate is considered a less load-dependent measurement of myocardial contractility but requires high temporal resolution, which is a technical limitation when using STE.[53] Strain imaging based on STE is angle-independent and is not influenced by cardiac translation. Strain imaging allows the assessment of both regional or segmental deformation and global deformation, which is an averaged value. For the LV, the most common measurement is global longitudinal strain that averages segmental values over 18 segments. It has been demonstrated to be a highly reproducible measure of LV systolic function that detects changes even before the LV EF changes and also has additional prognostic value in different diseases. For the RV, guidelines on how to measure RV longitudinal strain have been published, and these suggest the use of RV free wall strain as a measure for RV systolic function from an RV-focused 4-chamber view (Fig. 2).[54] Over the past decade, in the adult population, normal values for RV strain and strain rate have been published.[55–57] In adults, an absolute value of >20% is considered normal.[4] In adults, RV strain has been used to assess RV function in CHD, systemic RVs, cardiomyopathies, and PH.[3,4,57–61] In recent years, specific software packages have been developed that facilitate clinical integration of RV strain into clinical practice. Normal paediatric values are in the same range as adult values but are based on relatively smaller groups of patients (Table 3).[62] Recent paediatric data have demonstrated that RV strain has additional prognostic value in patients with PH.[63] Absolute RV strain values <15% are associated with poor outcomes.[63] RV strain is an emergent technique, and in some centres the routine

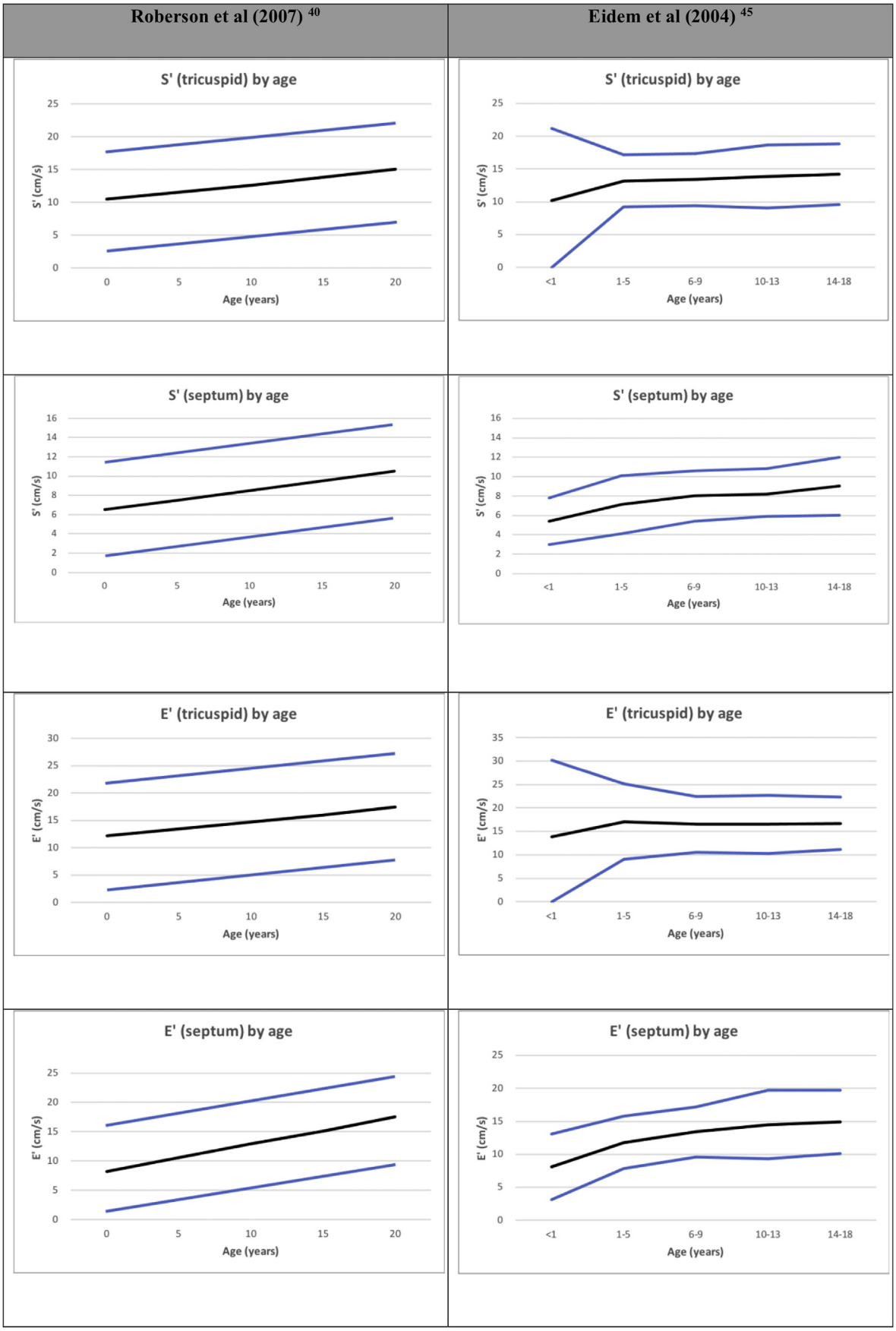

Figure 3. Tricuspid valve (TV) S′ by age.[40,45] TV S′ and E′ of the right ventricular free wall and medial wall. Normalized by age from Roberson et al.[40] and Eidem et al.[45] **Black line**: mean, **blue line**: +2SD.

Table 3. Published RV strain for paediatrics and adults

	Levy 2014*[152] (paediatrics)	Cantinotti 2018[†,62] (paediatrics)		Muraru 2022[57] (adult)		
RV global longitudinal strain	−29.03% (−26.54% to −31.52%)	31 d to 24 mo	−25.4% ± 3.9%	Fine et al., 2013[110]	−21.7% ± 4.2%[‡]	−20.4% ± 3.2%[†]
				Chia et al., 2014[111]	−27.3% ± 3.3%[‡]	−22.4% ± 2.4%[†]
		2-5 y	−25.9% ± 4.0%	Morris et al., 2016[112]	−28.5% ± 4.8%[‡]	−24.5% ± 3.8%[†]
				Muraru et al., 2016[113]	−30.5% ± 3.9%[‡]	−25.8% ± 3.0%[†]
		5-11 y	−25.8% ± 4.7%	McGhie et al., 2017[114]	−25.4% ± 5.0%[‡]	NR
				Park et al., 2018[38]	−26.4% ± 4.2%[‡]	−21.5% ± 3.2%[†]
		11-18 y	−25.0% ± 4.1%	Addetia et al., 2021[115]	−28.3% ± 4.3%[‡]	−25.4% ± 3.8%[†]
RV apical longitudinal strain	−29.16% (−25.33% to −32.99%)					
RV mid-ventricular longitudinal strain	−32.33% (−29.24% to −35.42%)					
RV basal longitudinal strain	−33.53% (−29.42% to −37.64%)					

Levy: mean (5th %ile to 95th %ile); Cantinotti: mean ± SD; Muraru: mean ± 2SD.
NR, not reported; RV, right ventricle; SD, standard deviation.
* Combined global full RV myocardial strain and global RV free wall strain.
† Data derived from full RV myocardial strain.
‡ Data derived from global RV free wall strain.

assessment of RV strain has been incorporated in clinical scanning protocols for patients at risk for developing RV dysfunction such as paediatric PH, TOF patients, and systemic RVs such as in patients with HLHS.

3D echocardiogram EF and strain. Three-dimensional echocardiography (3DE) allows for full-volume data acquisition for the assessment of volume, EF, and strain. It has been shown to be more reliable and reproducible in assessing all these indices for the LV than 2D echocardiography.[4,64,65] The 3DE assessment of the RV compared with MRI was found to be accurate, reproducible, and faster for quantitation of RV volumes and EF.[66] 3DE RV strain and RV EF have also shown prognostic value in a variety of cardiac conditions.[67−69] However, 3DE of the RV requires full-volume, high frame rate acquisition that can be difficult due to the RV orientation and shape, which limits the imaging windows, particularly in dilated RVs and postoperative patients. Without clear delineation of endocardial borders, 3D data can significantly vary on serial measurements. If 3DE is applied clinically, focused 4-chamber imaging of the RV with the optimization of myocardial definition and elongation of the RV is required. 3DE RV EF is an integral component in assessing adult right heart disease and has been incorporated into paediatric echocardiography laboratories for some diagnoses as the software continues to improve [4,70] Paediatric 3D strain is an ongoing area of study, with recent publications on 3D area strain.[71]

RV systolic pressure. RV systolic pressure is a measure of the peak systolic pressure generated by the RV. It is calculated based on continuous wave Doppler of TR, measuring the trans-TV pressure difference between the RA and RV. The peak pressure generated plus the estimated right atrial pressure is the reported RV systolic pressure. RV systolic pressure is most commonly used to assess pulmonary systolic pressures in the context of an unobstructed RV outflow, or the degree of RV outflow obstruction in the context of normal RV systolic function. RV systolic pressure can also be used to assess RV systolic function when there is an atretic outflow. In this situation, if the RV systolic pressure is low, it is indicative that the RV is unable to generate sufficient pressure; if the RV systolic pressure is at least 1/3 systemic, the RV is generating normal pressure and the function is therefore normal. This method of assessing RV function has been useful in the prognostication of neonatal Ebstein malformation with functional or anatomic pulmonary atresia.[72,73]

Clinical utility of RV systolic function parameters. Although RV systolic function is generally assessed qualitatively in clinical practice, relatively simple quantitative measures of RV function are easy to incorporate in routine clinical practice, especially in patients at risk for developing RV dysfunction. For paediatric echocardiography, RVFAC would be the easiest measurement to include, which is independent of age. TAPSE and TDI TV S′ are easy and reproducible methods that can be used for serial assessment, but their age and size dependence must be considered when used in children. RV strain is an emerging technique that could be relatively easily implemented given the recent evolutions in

Table 4. Utility of RV measures

Test	RV function	Window dependent	Geometry dependent	Reproducibility	Load dependent	Heart rate dependent	Age dependent	Angle dependent
RVFAC[4]	Regional	Yes	Yes	+	++	−	−	−
TAPSE[35]	Regional	No	No	++	+++	−	++	++
TV S′[40,41]	Regional	No	No	++	+++	+	++	++
RV strain[4]	Regional or global	Yes	Yes	+	+	−	+	−

RV, right ventricle; RVFAC, RV fractional area change; TAPSE, tricuspid annular plane systolic excursion; TV, tricuspid valve.

software applications. Table 4 summarizes several simple and reproducible methods of assessing RV systolic function.

A practical approach to assessing RV systolic function: Simple and reproducible methods of assessing RV systolic function should be incorporated into routine echocardiographic assessment, including RVFAC, TAPSE, and RV strain measurements for patients at risk of developing RV dysfunction.

Right ventricular diastolic function

Multiple acute and chronic conditions can influence RV diastolic function, including chronic pressure and volume loading, pulmonary lung disease, LV dysfunction, and cardiomyopathy. RV diastolic function is however difficult to assess, and there are no guidelines available for assessing RV diastolic function. RV hypertrophy can be associated with abnormal RV relaxation and RV fibrosis that can affect RV compliance and stiffness. The different components of RV diastolic function can be assessed using an integrated approach involving multiple parameters; however, we must keep in mind that there are significant limitations and pitfalls. RV diastolic function has been relatively poorly studied with limited validation of the echocardiographic measurements. The impact of respiration on RV filling and highly variable loading conditions in right-sided heart disease further complicates the interpretation of RV diastolic parameters. Hopefully, newer imaging modalities will allow us to better delineate diastolic dysfunction in the future.[74]

RA size. Chronically elevated right atrial (RA) pressure will result in RA dilatation, and thus, RA size can be used as a marker of RV diastolic dysfunction in the absence of a significant atrial L-R shunt or significant TV disease. The measurement of RA size can be performed from the apical RV-centric view (Fig. 4). RA area is performed by planimetry of the RA endocardium (excluding superior vena cava, inferior vena cava, RA appendage, and area between TV leaflets and annulus) at end ventricular systole, when the RA is at its largest volume.[4] At the same point in the cardiac cycle, the RA long axis is measured from the centre of the tricuspid annulus to the superior RA wall, parallel to the interatrial septum.[4] The mid-RA minor axis is from the mid-RA free wall to the interatrial septum, perpendicular to the RA long axis.[4] Right atrial volume can be calculated from single plane area-length (RA volume = 0.85(RA area)^2/major dimension). RA dimensions can be falsely enlarged in cases of chest and thoracic spine deformities. Right atrial area is an easily obtained, good, and simple screening tool for suspected RV diastolic dysfunction.

IVC diameter. IVC size, IVC collapsibility with inspiration, and hepatic Doppler a-wave can provide estimates of RA pressure. IVC dilation with poor respiratory variation and increased hepatic a-wave can indicate increased RA pressure.[3]

Tricuspid valve inflow and TV tissue Doppler imaging. TV inflow E, A, E/A ratio can be measured from the apical 4-chamber or RV-centric views (Table 5). Typically, TV inflow patterns are more difficult to technically optimize and are

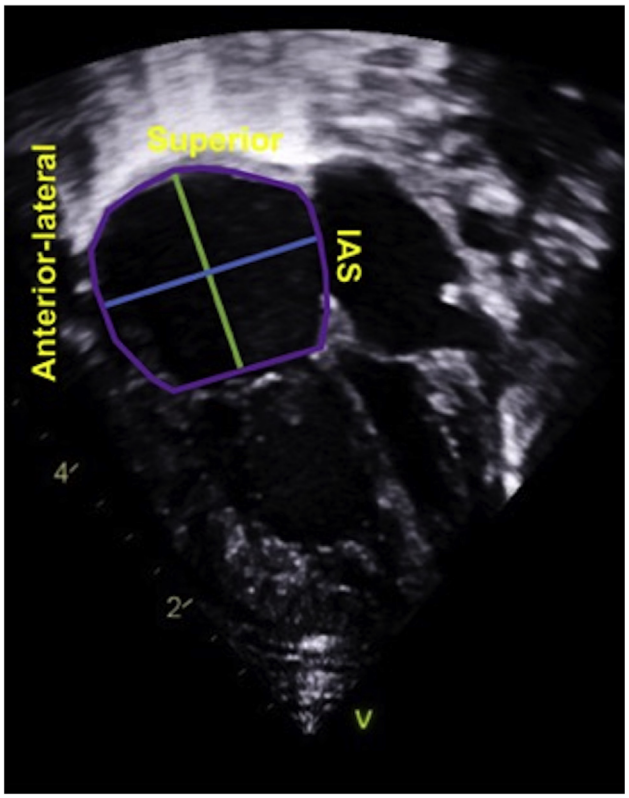

Figure 4. Right ventricular (RA) measurements.[28] Right atrial area (area enclosed by the **purple line**) is performed at end ventricular systole by tracing from the tricuspid valve annular plane, along the interatrial septum (IAS), superior RA, and anterolateral wall. Right atrial long axis (major dimension, **green line**) is measured from the mid-tricuspid valve annulus to the superior right atrial wall, parallel to IAS. Right atrial transverse axis (minor dimension, **blue line**) is measured from the mid-anterolateral wall to the mid-IAS. Right atrial volume = 0.85(RA area)^2/(green major dimension).

Table 5. RV diastolic parameters, TV inflow and RV free wall

Age	Study	E (cm/s)	A (cm/s)	E/A	E′ (cm/s)	A′ (cm/s)	S′ (cm/s)	E/E′
Preterm	Johnson et al., 1988[154]	46.0 ± 11.0	70.0 ± 14.0	0.88 ± 0.19	NR	NR	NR	NR
	Ciccone et al., 2011[155]	38.2 ± 7.3	48.9 ± 8.5.0	0.78 ± 0.13	NR	NR	NR	NR
Term (2-5 d)	Johnson et al., 1988[154]	58.0 ± 16.0	81.0 ± 15.0	0.78 ± 0.25	NR	NR	NR	NR
	Ciccone et al., 2011[155]	47.9 ± 8.6	54.9 ± 8.7	0.88 ± 0.17	NR	NR	NR	NR
<1 y	Eidem et al., 2004[45]	53.3 ± 12.3	53.2 ± 13.0	1.01 ± 0.38	13.8 ± 8.2	9.8 ± 2.4	10.2 ± 5.5	4.4 ± 2.3
	Vorhies et al., 2014[156]	NR	NR	1.08 ± 0.45	9.2 ± 3.1	8.8 ± 1.3	8.3 ± 1.8	6.2 ± 1.5
	Rafeiyian et al., 2006[157]	NR	NR	NR	13.11 ± 3.30	11.89 ± 2.67	10.00 ± 0.89	NR
1-5 y	Eidem et al., 2004[45]	61.6 ± 12.5	48.3 ± 12.3	1.27 ± 0.31	17.1 ± 4.0	10.9 ± 2.7	13.2 ± 2.0	3.8 ± 1.1
	Rafeiyian et al., 2006[157]	NR	NR	NR	17.07 ± 1.77	12.13 ± 1.65	13.7 ± 2.34	NR
	Swaminathan et al., 2003[158]	NR	NR	NR	14.7 ± 2.1	9.5 ± 2.2	11.8 ± 1.4	NR
6-9 y	Eidem et al., 2004[45]	60.5 ± 13.9	42.4 ± 10.8	1.49 ± 0.40	16.5 ± 3.0	9.8 ± 2.7	13.4 ± 2.0	3.6 ± 0.8
	Rafeiyian et al., 2006[157]	NR	NR	NR	16.53 ± 1.59	11.69 ± 1.88	13.80 ± 2.12	NR
	Swaminathan et al., 2003[158]	NR	NR	NR	16.1 ± 2.8	7.7 ± 1.5	12.5 ± 2.2	NR
10-13 y	Eidem et al., 2004[45]	59.6 ± 11.4	39.2 ± 11.3	1.61 ± 0.47	16.5 ± 3.1	10.3 ± 3.4	13.9 ± 2.4	3.5 ± 1.4
	Rafeiyian et al., 2006[157]	NR	NR	NR	17.00 ± 1.50	13.33 ± 1.73	14.10 ± 1.27	NR
	Swaminathan et al., 2003[158]	NR	NR	NR	14.6 ± 2.2	8.2 ± 1.5	12.3 ± 1.5	NR
14-18 y	Eidem et al., 2004[45]	60.4 ± 10.9	34.5 ± 11.2	1.88 ± 0.56	16.7 ± 2.8	10.1 ± 2.6	14.2 ± 2.3	3.7 ± 1.0
	Swaminathan et al., 2003[158]	NR	NR	NR	15.6 ± 3.1	7.8 ± 2.3	12.5 ± 1.8	NR
Overall (0-18 y)	Eidem et al., 2004[45]	59.2 ± 12.4	43.3 ± 13.5	1.47 ± 0.53	16.1 ± 4.7	10.2 ± 2.8	13.0 ± 3.4	3.8 ± 1.4
	Groner et al., 2013[159]	46.51 ± 8.26	37.22 ± 11.16	1.37 ± 1.22	14.98 ± 4.17	10.56 ± 2.13	12.16 ± 3.31	3.23 ± 1.01
	Vorhies et al., 2014[156]	NR	NR	1.66 ± 0.62[5]	13.0 ± 3.6[5]	8.4 ± 2.3	11.6 ± 2.8[5]	4.9 ± 1.4
	Rafeiyian et al., 2006[157]	NR	NR	NR	16.51 ± 2.14	12.06 ± 1.87	13.40 ± 2.34	NR
	Swaminathan et al., 2003[158]	NR	NR	NR	15.2 ± 2.6	8.5 ± 2.0	12.6 ± 1.9	NR

Values expressed as mean ± 2SD.
NR, not reported; RV, right ventricle; TV, tricuspid valve.

highly influenced by respiration as inspiration will be associated with a significant increase in inflow through the TV.[3] This makes the inflow velocities and patterns more variable compared with mitral valve inflow patterns. TDI velocities of the TV lateral annulus allow measurement of E′, A′, and calculated E′/A′ ratio.[4] RV TDI velocities are less influenced by respiration than TV inflow Dopplers (Table 5, Fig. 3). When assessing RV TV inflow and TDI velocities, it is important to consider the impact of age, heart rate, and preload. Both inflow velocities and TDI velocities change with age and also heart rate. The E/A ratio increases with age and preload and decreases with tachycardia.[4,74,75] Increased preload increases E > A and bradycardia increases A > E, with both increasing the E/A ratio.[76] Decreased preload and tachycardia decreases the E/A ratio. Exercise increases both E and A; however, with diastolic dysfunction, there is a failure of

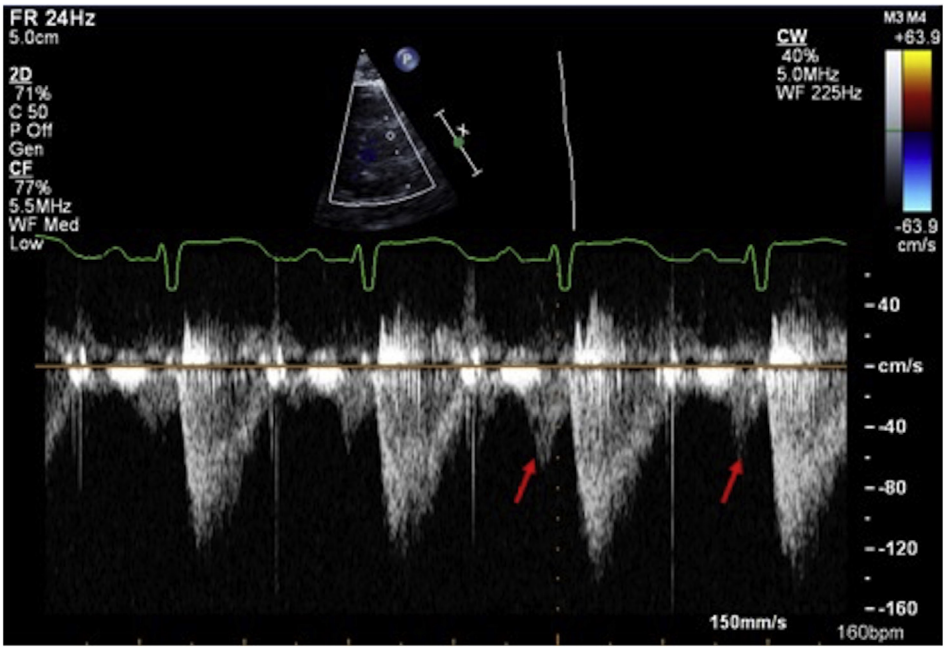

Figure 5. Right end-diastolic forward flow by echocardiography.[87] Restrictive physiology of the right ventricle can be assessed by pulse wave Doppler of the main pulmonary artery mid-way between the pulmonary valve and pulmonary artery bifurcation. A restrictive right ventricular has antegrade end-diastolic flow in the MPA from atrial contraction (**arrow**).

rapid early filling, so there is a greater dependence on atrial contraction with increased RA pressure.[77] TDI is less load dependent than TV inflow, so a reduction in preload causes an equal decrease in E′ and A′ and therefore there is an unchanged E′/A′.[78] Tissue Doppler can help in detecting underlying relaxation abnormalities of the RV but, given the age and heart dependence, can be difficult to interpret.

RA strain. Alterations in atrial strain can be a precursor to ventricular diastolic dysfunction. Left atrial strain has been useful in the assessment of LV diastolic dysfunction in a multitude of paediatric conditions.[79–81] Right atrial strain is an emerging technique to assess RV stiffness. In recent years, there has been increasing evidence that RA strain correlates with right heart haemodynamics and prognostication in heart failure and PH.[82–84] RA strain is obtained by speckle tracking of the RA in the apical 4-chamber view to assess RA longitudinal motion.[85] There are 3 components of RA strain: (1) active strain, (2) conduit strain, and (3) reservoir strain. The normal RA acts as a distensible reservoir during ventricular systole (reservoir function), a passive conduit for systemic venous flow during early ventricular diastole (conduit function), and a pump in late ventricular diastole (active function). Each contributes to effective RV filling. Clinical utility of this method in paediatrics is limited by the ability to track a thin-walled RA, the assumption that the right atrial wall fibres are aligned longitudinally, and the influence of RA dilation on the assessment of RA function. However, with future technical advances, the assessment of RA strain may become a strong surrogate for assessing RV diastolic function in paediatrics.

Late diastolic antegrade flow in pulmonary artery. RV restrictive physiology is when the RV has increased myocardial stiffness and decreased compliance, leading to a fast increase in RV diastolic pressure during early filling and increased RV end-diastolic pressure. At the end of diastole, during atrial contraction, this can result in a higher RV diastolic pressure compared with the diastolic PA pressure, which results in opening the pulmonary valve with antegrade pulmonary blood flow during atrial contraction. In healthy individuals, this can even occur during inspiration. When antegrade flow is seen throughout the respiratory cycle in the main PA, elevated RV end-diastolic pressure or increased RV stiffness should be considered, if there is no significant pulmonary insufficiency or RV dilation.[86] By echocardiography, this can be assessed using pulse wave Doppler just distal to the pulmonary valve (Fig. 5).[87]

Clinical utility of RV diastolic function parameters. Paediatric RV diastolic function studies have used heterogeneous methodologies, and results for normal values are limited by study size. Variation in nomograms depends on how studies factor in the relationship of the velocities to growth and age. The clinical utility of RV diastolic parameters has also been limited, with most reports predominately focused on the repaired TOF population.[88,89] The most clinically useful screen is to assess RA size, TV inflow, and RV TDI patterns in conjunction with hepatic Doppler and IVC collapsibility, as markers of RA pressure. In general, in the first few months of life, TV E-wave increases rapidly as RV relaxation improves, and tricuspid TDI E′ and A′ velocities are decreased and there is inversion of the E/A and E′/A′ pattern (Table 5).[45,90] Stable values are reached at 1-2 years of age.[45,90] After 3 years of age, the diastolic patterns are similar to adults with values increasing with growth and age.[45,90]

A practical approach to assessing RV diastolic function: Assess RA size, TV inflow, and RV TDI pattern in conjunction with hepatic Doppler and IVC collapsibility, as markers of RA pressure.

Assessing TV Function

In the normal heart, the tricuspid annulus is more compliant than the mitral annulus and therefore is more likely to dilate as the RV dilates. *In vitro* work has demonstrated that TR occurs starting at 40% of annular dilatation, whereas it only occurs at 75% annular dilatation for the mitral valve.[91] This study also demonstrated that abnormal papillary muscle position can contribute to causing TR.[91] When evaluating TR, a detailed description of the different contributing mechanisms is required. These include (1) annular dilatation, (2) leaflet prolapse, (3) leaflet tethering with restricted motion, and (4) leaflet structural abnormalities (clefts, additional scallops, etc.) and abnormalities of the subvalvar apparatus including papillary muscle insertion. The TV has significant variability even within normal TVs,[11] making the assessment of TR mechanisms by 2D echocardiography alone limited.[92] Concomitant 3DE can provide additional information regarding the mechanisms of TR.[93–95] In paediatrics, this can be performed by transthoracic imaging from the 4-chamber and/or subcostal view.[96]

A practical approach to assessing TV function: Concomitant information regarding RV function can be provided through the assessment of TR mechanisms, including TR grade and location, TV annular size, leaflet morphology, leaflet prolapse/tethering, and papillary muscle position. This is most optimally assessed through the use of both 2D and 3D echocardiography.

Assessing the RV Under Differing Loading Conditions

The RV is constructed to efficiently manage a low-pressure and highly compliant pulmonary circulation. When placed under altered haemodynamics, this configuration becomes less effective and changes occur depending on the type and length of exposure to pressure overload and volume overload.

Pressure-loaded RV

RV pressure loading is relatively common in CHD—occurring in severe pulmonary stenosis, RV-PA conduit stenosis, branch PA stenosis, cyanotic TOF, single systemic RV, and PH. In contrast to the LV, a normal RV is extremely sensitive to an acute increase in afterload with a quick decrease in RV output in response to changes in PA pressure. This explains why RV dysfunction is commonly detected in acute pulmonary embolism if associated with

Echo measure	Figure	How to Measure
Right ventricular systolic pressure	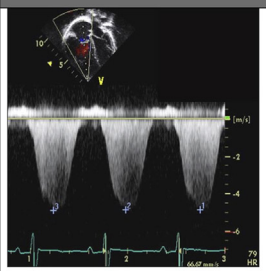 **Normal: <1/3 systemic**	RVSp = Peak TR jet velocity +RAp • Any view parallel to TR jet • Continuous wave Doppler of TR • Underestimated if poor RV systolic function • Unreliable if there is RVOT or branch pulmonary artery obstruction • Contaminated by LV-RA shunts
Mean PA pressure	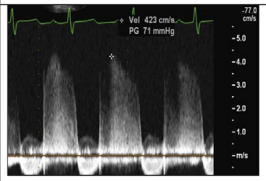 **Normal: mean PAP <25mmHg**	Mean PAp = Peak PI + RVEDp • Any view parallel to PI jet • Continuous wave Doppler of PI • Accurate only if < mild+ PI
PA acceleration time	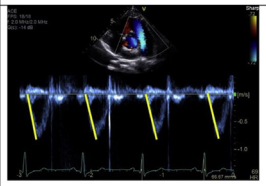 **Normal: >100ms**	PA acceleration time = time from onset of ejection to peak (Yellow line) • Parasternal short axis • Pulse wave Doppler in MPA, distal to pulmonary valve • Correlates with contractility and inversely to vascular compliance
RV/LV diameter ratio	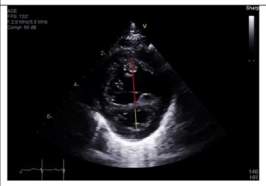 **Normal <1 (do not use in L-R shunts)**	RV/LV ratio = RV diameter (Red Line): LV diameter (Green Line) • Parasternal short axis of RV and LV at LV papillary muscle level, at end systole (Do not include RVOT as IVS will naturally appear flat) • Do not measure if left to right shunt
LV eccentricity index	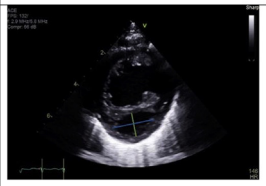 **Normal diastolic EI <1**	EI = D2/D1 ○ D1: LV dimension perpendicular to septum (Green Line) ○ D2: LV dimension parallel to septum (Blue Line) • Parasternal short axis, papillary muscle level • Can be measured at end-systole and diastole • End-diastole EI >1 associated with poor outcomes
TAPSE, TV S', RVFAC, RV free wall strain and strain rate, RV and RA size	See Figures 2 and 4	See Figures 2 and 4

RV: Right ventricle, RVSp: RV systolic pressure, TV: Tricuspid Valve, TR: Tricuspid Regurgitation, LV: Left Ventricle, RA: Right atrium, RVEDp: RV end diastolic pressure, PAp: Pulmonary artery pressure, RVOT: RV outflow tract, IVS: Interventricular Septum, EI: Eccentricity Index, PI: Pulmonary Insufficiency, TAPSE: Tricuspid annular plane systolic excursion, RVFAC: RV Fractional Area Change, RVOT: RV outflow tract

Figure 6. Additional pulmonary hypertension (PH) assessment.[28,105,160]

increased PA pressure. Chronic pressure loading results in hypertrophic remodelling and changes in myocardial gene expression patterns.[7] Over time, the RV becomes less dependent on longitudinal shortening and more on transverse wall motion.[7] This hypertrophic RV adaptation to chronic pressure loading has been observed in transposition of the great arteries (TGA) after atrial switch operation, congenitally corrected transposition of the great arteries (ccTGA), HLHS, and idiopathic PH.[97,98] When this adaptation gets exhausted and contractility can no longer increase to match afterload, the process becomes maladaptive leading to RV dysfunction.[7] There are different types of pressure loading: (1) increased RV pressure associated with PH, (2) increased RV pressure associated with RV outflow tract obstruction, and (3) increased RV pressure associated with the RV functioning as the systemic ventricle.

Pulmonary hypertension. Echocardiography is used in the diagnosis and follow-up of children with suspected or confirmed PH. Systematic assessment with a transthoracic echo protocol increases the identification of children with PH and can decrease the need and frequency of more invasive testing such as MRI or catheterization. Multiple prognostic echocardiographic measures in adults with PH have been published, including RA size, RA strain, RV longitudinal strain, septal position, TAPSE, and pericardial effusion.[99–104] Raymond et al.[101] demonstrated a strong correlation of indexed RA area, septal shift (measured by eccentricity index), and pericardial effusion with death or transplant. RV and LV longitudinal strain, RV systolic pressure, TAPSE, and RVFAC correlate well with 6-minute walking distance, whereas RV longitudinal strain was also associated with hospitalization and death.[102] One of the largest publications assessing risk factors for mortality in pulmonary arterial hypertension found PH patients with PA dilation, moderate-to-severe TR, decreased RVFAC, and pericardial effusion have poor prognosis.[103] ***Paediatric literature, although smaller in number and size, show similar findings, with 3DE RV EF, 3D volumes, RVFAC, RV free wall strain, and RA strain predicting PH outcomes.[70] The PH population requires serial and complete PH-focused imaging of all these components (Fig. 6).[28,105]***

> **A practical approach to assessing RV function in PH:** Systematic serial assessment including estimation of RV systolic pressure, estimation of mean PA pressure (PI jet velocity by CW Doppler), RVFAC, TAPSE, RV free wall longitudinal strain, RV/LV diameter ratio, LV eccentricity index, RA and RV size, and LV function.

RV outflow tract obstruction/pulmonary stenosis. RV remodelling differs in pulmonary stenosis compared with PH. Although in PH the hypertrophic response can result in progressive RV dysfunction, the hypertrophied RV in pulmonary stenosis (PS) is generally well tolerated. Driessen et al.[43,106] demonstrated that RV output and RV EF are generally well preserved in patients with PS in contrast to those with PH. Although systolic function is well preserved, RV hypertrophy and RV fibrosis may result in the development of RV diastolic dysfunction and development of RV restrictive physiology.[107] In current eras, PS is typically treated in a timely manner by balloon valvuloplasty with good long-term outcomes. ***In the assessment of patients with PS or RV outflow tract obstruction, the evaluation of RV systolic function is important, as RV systolic dysfunction can occur in cases of PS progression, especially in younger children. Additional analysis of progressive TR and RV diastology, in particular RV restrictive physiology, is also needed.***

> **Practical approach to assessing RV function in RV outflow tract obstruction:** (1) Pulmonary outflow gradient; (2) RV diastolic function including RA size, PW of TV inflow, antegrade flow in PA during atrial contraction; (3) RV systolic function including TAPSE and RVFAC; and (4) severity of TR + gradient.

Transposition of the great arteries after atrial switch + corrected transposition of the great arteries. Although systemic RVs (TGA post-atrial switch and ccTGA) can initially compensate for the chronic pressure loading, the occurrence of RV dysfunction during follow-up is an important concern for both groups. Systemic RV mechanics have been described as becoming more LV-like with a more predominant circumferential over longitudinal free wall shortening, with no torsion.[108] As the RV fails, it dilates and can become more spherical, which can contribute to the development of LV dysfunction from the change in ventricular-ventricular interactions.[109] In atrial switch patients, the late development of PH contributes to the LV dysfunction and overall haemodynamic deterioration.[110,111] Monitoring of TR progression in both lesions is important but for different reasons. In atrial switch patients, progression of TR is secondary to progressive RV dilatation and RV dysfunction. On the other hand, in ccTGA, RV dysfunction is often intrinsic to associated TV anomalies and surgical treatment of TR is needed before RV function further declines.[109] ***The serial assessment of RV parameters is of key importance for these patient groups as the development of progressive RV dysfunction is of prognostic importance. RV assessment includes: (1) assessment of RV size (TV annulus dimension and RV area), (2) RV systolic parameters including RVFAC, TAPSE, and RV strain, (3) severity of TR, and (4) LV function.***

> **Practical approach to assessing RV function in TGA/ccTGA**: RV size, TAPSE, RVFAC, RV strain (longitudinal), LV function, and degree of TR.[106]

Hypoplastic left heart syndrome. In HLHS, as the RV adjusts to increased volume and pressure, changes occur in RV deformation, RV size and shape, and TV mechanics, with each component influencing each other. This ultimately impacts the long-term performance of the RV. Similar to other conditions where the RV functions as the systemic ventricle, in HLHS, the RV adapts mechanically with an increase in circumferential deformation and a relative decrease in

longitudinal deformation with increased reliance on atrial contraction for ventricular filling.[112,113] In patients with HLHS, the assessment of RV size and function is critical as the development of RV dysfunction has significant prognostic implications at any stage of HLHS palliation. The geometry of the LV can also significantly influence RV function. Depending on the size of a hypoplastic and/or hypertrophied LV, the RV can develop an apical bulge with decreased RV strain.[114] TR is also a critical part of HLHS assessment, as alterations in ventricular geometry can also alter TV and RV mechanics.[13,115] ***Serial follow-up studies in patients with HLHS have suggested measurements of RV size (RV area), RV function (RVFAC and RV strain), and TR severity to be consistently proven prognostic factors.[2,95,116–119] The TV is often abnormal in HLHS, and it is important to describe the TV morphology and TV annulus. Progressive RV dilatation and dysfunction often contribute to progression of TR.***

Practical approach to assessing RV function in HLHS: (1) RV size (TV annulus and RV area), (2) RV function (RVFAC, RV longitudinal strain), and (3) TR severity.

Volume-loaded RV

RV volume loading is generally tolerated better than RV pressure loading, probably related to the thinner and more compliant RV myocardium. The RV adjusts to the volume by dilating and then undergoing eccentric hypertrophy.[7]

RV contraction is typically preserved but can become compromised with chronic loading, as can be seen in long-standing large ASDs and post-repair TOF with significant pulmonary insufficiency (PI).[46] The LV develops simultaneous dysfunction with decreased compliance and EF from septal displacement and changes in LV geometry when RV biomechanics are altered.[7] This can increase morbidity and mortality, especially when superimposed with pressure overload and marked RV enlargement.[7]

Atrial septal defects. Right atrial and ventricular enlargement and diastolic flattening of the interventricular septum are the predominant echocardiographic features of a haemodynamically significant ASD. Typically eccentric remodelling associated with a haemodynamically significant ASD results in normalization of RV systolic parameters including RVFAC, TAPSE, RV strain, and strain rate.[52,120] Several studies have consistently demonstrated preserved longitudinal strain in the RV free wall, but higher apical strain, suggesting that RV apical contraction contributes to the increased RV output.[46,121] After ASD closure RV systolic parameters typically acutely decrease, which reflects the effect of acute volume unloading and not of decreased RV contractile function.[52] With reverse RV remodelling, RV functional parameters normalize over time.[120] ***Several considerations should be made when assessing RV function in the presence of an ASD. (1) As RV size is typically used to decide on the need for ASD closure, RV size is an intrinsic part of an ASD assessment.[122] (2) As ASDs can be associated with PH, the assessment of RV pressure is essential. (3) RV diastolic dysfunction typically does not develop with ASDs unless there is associated RV hypertension with concentric hypertrophy.[46,123] (4) RA size in patients with ASDs is reflective of the left to right shunt rather than RV diastolic dysfunction. (5) Typically, RV dilatation in paediatric patients with ASDs does not result in significant TR; therefore, if moderate-to-severe TR is present, TV morphology needs to be studied in detail. (6) In older patients with ASDs, the assessment of LV diastolic function is important, as its presence can result in a significant increase in LV filling pressures after ASD closure.[124] However, the presence of an ASD can complicate the interpretation of LV diastolic parameters by echocardiography. As such, a complete assessment of LV filling pressures can sometimes only be done with balloon occlusion before ASD closure.[124]***

Practical approach to assessing RV function in ASDs: (1) RA and RV size, (2) RVFAC, (3) TR severity, (4) RV systolic pressure to ensure that the right-sided dilation is secondary to the ASD rather than underlying PH.

Postoperative TOF repair with pulmonary insufficiency. Pulmonary insufficiency after TOF repair typically results in progressive RV dilatation in the first years after surgery. The pulmonary regurgitant volume determines the degree of RV dilatation long-term, and this is influenced by RV diastolic function. A stiffer RV is associated with a lower regurgitant volume as higher diastolic pressures limit the backflow from the pulmonary circulation, resulting in less RV dilation.[84,125] Thus, there is a direct interaction between diastolic properties and RV size in this patient cohort, demonstrating the importance of assessing diastolic functional parameters in postoperative TOF patients. ***This consists of assessing RA size, TV inflow, and PA flow with antegrade flow in the PA during atrial contraction throughout the respiratory cycle as indicating RV restrictive physiology.***

Once eccentric remodelling has occurred, the RV size should remain relatively stable, especially in the adult TOF cohorts. Progressive RV dilation suggests progressive RV dysfunction.[126] ***Therefore, monitoring of RV size is essential in this patient cohort. This could be done by assessing RV area or 3D RV volumes.[127]*** MRI measures of RV volumes remains the gold standard for assessing RV health, but over the years several echocardiographic parameters have been used for serial monitoring, ***RV end-diastolic and systolic area and volumes (from 4-chamber), and RV dimension in short axis have shown good correlation with MRI-derived RV volumes.[127]*** An indexed RV end-diastolic area of >20 cm^2/m^2 can predict the RV volume >180 mL/m^2.[128] New advances in 3DE have provided fast, accurate, and reproducible acquisition when compared with MRI, which may be used for clinical use in the future.[127]

Ultimately, RVs after TOF repair are prone to developing RV dysfunction. In recent large cohort studies, decreased RV function has been identified as one of the main contributors to adverse clinical outcomes. ***Echocardiographic parameters that can be monitored include RVFAC that in TOF has good correlation***

with MRI RV EF.[129] ***RV longitudinal strain is another quantitative parameter that can be monitored over time.***[130] RV strain is influenced by RV volume, PI fraction, and possible residual RV outflow obstruction. The RV in postoperative TOF with PI adapts differently than in patients with ASDs. Typically, RV free wall strain and strain rate is reduced and is worse towards the apex compared with the base.[46,57] The larger the RV size, the greater the decrease in longitudinal strain.[46,57] Those with worse PI had higher strain than those with minimal PI.[57] RV strain correlates with MRI RV EF[131] and exercise performance.[107] TAPSE and RV TDI S′ are influenced by RV wall tethering that is common in the postoperative state, which makes a single assessment not representative of global RV function after TOF repair.[38] However, TAPSE can be tracked over time and decreasing TAPSE could be a marker for a decrease in RV function.[131]

As the RV dilates, it can also impact LV function, with septal shift, decreased LV filling, and increased LV end-diastolic filling pressures.[132] ***Decreased LV function, as indicated by decreased LV EF, LV GLS, and decreased LV circumferential strain, has also been identified as an important risk factor for adverse outcomes in the TOF patient cohort.***[57]

TR can be associated with RV dilatation, RV dysfunction, and can be a consequence of VSD closure as the patch can interfere with TV function.[133] Associated moderate-to-severe TR in the presence of severe PI adds to RV volume loading and typically is clinically not well tolerated, which can lower the threshold for reintervention.[133] ***A careful assessment of TV function and RV systolic pressure is part of the postoperative TOF echocardiography.***

Practical approach to assessing RV function in repaired TOF: (1) IVC size and respiratory variation, hepatic Doppler, RA size and identification of restrictive physiology; (2) RV size (RV area as the best approximation of RV volumes); (3) RV function with RVFAC and RV free wall longitudinal strain. For patients with dilated RVs, 3DE can help with RV volume and RV EF quantification; (4) TV function.

Ebstein's anomaly. In Ebstein's anomaly (EA), an accurate assessment of cardiac chamber size and function is essential for risk stratification and management decisions before significant cardiomegaly or functional deterioration develops.[134,135] However, RV size and function can be difficult in EA due to the complex RV geometry, the presence of an atrialized RV, variable chamber dilation, and masked RV dysfunction secondary to volume overload.[136] The accurate echocardiographic assessment of RV size is limited due to the abnormal RV geometry. The Celmaier index can be used to describe severe EA, which occurs when the combined area of the RA and atrialized RV is larger than the total area of the functional RV, left atrium, and LV in the apical 4-chamber view at end diastole.[137] RV function in EA is also limited. 2D echocardiographic functional parameters do not correlate well with cardiac MRI.[138,139] Kuhn et al.[139] found that qualitative RV functional assessment and global longitudinal strain were the only 2 parameters that weakly correlated with MRI-derived RV EF. RV geometry and increased dependence on circumferential and radial contraction in volume-loaded hearts possibly contribute to the weak correlation.[140] RV diastolic parameters including the direction of atrial shunt and IVC and SVC size and Doppler pattern provide useful information regarding the degree of TR and the adequacy of the functional RV. The paradoxical motion of the interventricular septum and atrialized RV also alters LV geometry and function,[141,142] emphasizing the importance of monitoring LV function. Severe RV dysfunction is common early after the cone operation. After cone repair, 2D RVFAC and global longitudinal strain and 3DE RV volumes and function are closely correlated with MRI RV EF.[143]

Anatomic diagnosis of EA by echo is based on the septal leaflet apical displacement of greater than 8 mm/m^2 from the mitral valve anterior leaflet hinge point.[144] The posterior leaflet is also apically displaced in EA with TV inflow directed to the RV outflow tract (spiralling of the TV inflow). Adapted views of the TV include RV 2-chamber view (to visualize the posterior leaflet), RV apical 3-chamber view, short axis RV outflow tract view, and subcostal sagittal views. These views provide further information about leaflet motion, TV annulus, and degree of coaptation.[145–147] However, 2D echo is limited in its detailed assessment of EA tethering.[148–150] 3DE can add important additional information for preoperative planning to determine leaflet morphology, insertion and coaptation, mechanism and degree of TR or stenosis, and subvalvar apparatus.[151] Yet, 3D views can also be challenging related to complex 3D anatomy of the TV.

Practical approach to assessing RV function in Ebsteins Anomaly: (1) Qualitative RV function and global longitudinal strain, (2) qualitative RA, RV, LA, and LV size with the direction of atrial shunt, (3) degree of pulmonary outflow obstruction or regurgitation, (4) LV function with septal motion, and (5) TV anatomy and mechanism of TV regurgitation by 2D and 3DE.

Assessing the TV Under Differing Loading Conditions

TV function is closely linked with RV shape, size, and function.[109] It is also influenced by septal positioning that reflects the importance of the subvalvar apparatus and the papillary muscles in TV function. The normal morphological variability of the TV is further amplified in CHD with different pathologies affecting the right heart also resulting in morphological TV abnormalities and changes.[11] The mechanism and location of haemodynamically significant TR becomes even more complex in CHD compared with the normal TV. Recent studies have shown the ***utility of detailed 2D and 3D echocardiography together in assessing the morphology of the TV, mechanisms of TR, and in predicting future risks in some of the CHD populations.***[93–95]

Practical approach to assessing TR: (1) IVC size and hepatic Doppler, (2) RA size, (3) qualitative assessment of TR severity and quantification of tricuspid stenosis severity by pulsed waved and continuous wave Doppler assessment, (4) TR mechanisms: TV tethering/prolapse, TV annular size, and leaflet morphology by combined 2D and 3D echocardiography when TR is more than mild.

Conclusions

RV assessment is integral to the complete evaluation, management, and timing of intervention for many congenital heart lesions. The assessment of the RV can be difficult as there are no well-defined guidelines or normal values in paediatrics. RV assessments should include measuring the size of the right heart structures, quantification of RV systolic function, identification of RV diastolic function, and inclusion of TV functional analysis. Serial assessments can provide an overview of changes that occur over time, allowing for earlier identification of abnormalities, and can guide the clinician in helping to decide when interventions are warranted to prevent potential complications related to the development of RV dysfunction. A practical approach to each congenital lesion is suggested, which can be helpful in optimizing paediatric echocardiography laboratory resources by focussing on the measurements with the highest clinical relevance.

Ethics Statement

This article adhered to relevant research ethics.

Funding Sources

No funding was received for this study.

Disclosures

The authors have no conflicts of interest to disclose.

References

1. Knauth AL, Gauvreau K, Powell AJ, et al. Ventricular size and function assessed by cardiac MRI predict major adverse clinical outcomes late after tetralogy of Fallot repair. *Heart*. 2008;94:211–216.

2. Lin LQ, Conway J, Alvarez S, et al. Reduced right ventricular fractional area change, strain, and strain rate before bidirectional cavopulmonary anastomosis is associated with medium-term mortality for children with hypoplastic left heart syndrome. *J Am Soc Echocardiogr*. 2018;31:831–842.

3. Zaidi A, Knight DS, Augustine DX, et al. Echocardiographic assessment of the right heart in adults: a practical guideline from the British Society of Echocardiography. *Echo Res Pract*. 2020;7:G19–G41.

4. Rudski LG, Lai WW, Afilado J, Hua L, et al. Guidelines for the echocardiographic assessment of the right heart in adults: a report from the American Society of Echocardiography. *J Am Soc Echocardiogr*. 2010;23:685–713.

5. Dell'Italia LJ. The right ventricle: anatomy, physiology, and clinical importance. *Curr Probl Cardiol*. 1991;16:653–720.

6. Kawel-Boehm N, Maceira A, Valsangiacomo-Buechel ER, et al. Normal values for cardiovascular magnetic resonance in adults and children. *J Cardiovasc Magn Reson*. 2015;17:29.

7. Sanz J, Sanchez-Quintana D, Bossone E, Bogaard HJ, Naeije R. Anatomy, function, and dysfunction of the right ventricle. *JACC*. 2019;73:1463–1482.

8. Sengupta PP, Korinek J, Belohlavek M, et al. Left ventricular structure and function: basic science for cardiac imaging. *J Am Coll Cardiol*. 2006;48:1988–2001.

9. Kovacs A, Lakatos B, Tokodi M, Merkely B. Right ventricular mechanical pattern in health and disease: beyond longitudinal shortening. *Heart Fail Rev*. 2019;24:511–520.

10. Naeije R, Badagliacca R. The overloaded right heart and ventricular interdependence. *Cardiovasc Res*. 2017;113:1474–1485.

11. Tretter JT, Sarwark AE, Anderson RH, Spicer DE. Assessment of the anatomical variation to be found in the normal tricuspid valve. *Clin Anat*. 2016;29:399–407.

12. Nii M, Roman KS, Macgowan CK, Smallhorn JF. Insight into normal mitral and tricuspid annular dynamics in pediatrics: a real-time three-dimensional echocardiographic study. *J Am Soc Echocardiogr*. 2005;18:805–814.

13. Nii M, Guerra V, Roman KS, Macgowan CK, Smallhorn JF. Three-dimensional tricuspid annular function provides insight into the mechanisms of tricuspid valve regurgitation in classic hypoplastic left heart syndrome. *J Am Soc Echocardiogr*. 2006;19:391–402.

14. Takahashi K, Inage A, Rebeyka M, et al. Real-time 3-dimensional echocardiography provides new insight into mechanisms of tricuspid valve regurgitation in patients with hypoplastic left heart syndrome. *Circulation*. 2009;120:1091–1098.

15. Lopez L, Colan SD, Frommelt PC, et al. Recommendations for quantification methods during the performance of a pediatric echocardiogram: a report from the Pediatric Measurements Writing Group of the American Society of Echocardiography Pediatric and Congenital Heart Disease Council. *J Am Soc Echocardiogr*. 2010;23:465–495.

16. Rothstein ES, Palac RT, O'Rourke DJ, et al. Evaluation of echocardiographic derived parameters for right ventricular size and function using cardiac magnetic resonance imaging. *Echocardiography*. 2021;38:1336–1344.

17. Lai WW, Gauvreau K, Rivera ES, Saleeb S, Powell AJ, Geva T. Accuracy of guideline recommendations for two-dimensional quantification of the right ventricle by echocardiography. *Int J Cardiovasc Imaging*. 2008;7:691–698.

18. Mawad FD, Drolet C, Dahdah N, Dallaire F. A review and critique of the statistical methods used to generate reference values in pediatric echocardiography. *J Am Soc Echocardiogr*. 2013;26:29–37.

19. Colan SD. The why and how of Z scores. *J Am Soc Echocardiogr*. 2013;26:38–40.

20. Boston Children's Hospital Heart Center. Available at: https://zscore.chboston.org. Accessed December 15, 2021.

21. Lopez L, Colan S, Stylianou M, et al. Relationship of echocardiographic Z scores adjusted for body surface area to age, sex, race, and ethnicity: the Pediatric Heart Network Normal Echocardiogram Database. *Circ Cardiovasc Imaging*. 2017;10:e006979.

22. Lopez L, Frommelt PC, Colan SD, et al. Pediatric Heart Network echocardiographic Z-scores: comparison to other published models. *J Am Soc Echocardiogr*. 2021;34:185–192.

23. Koestenberger M, Nagel B, Ravekes W, Avian A, et al. Reference values and calculation of z-scores of echocardiographic measurements of the normal pediatric right ventricle. *Am J Cardiol*. 2014;114:1590−1598.

24. Wang S, Zhang Y, Chen S, et al. Regression equations for calculation of z scores for echocardiographic measurements of right heart structures in healthy Han Chinese children. *J Clin Ultrasound*. 2016;45:293−303.

25. Plante V, Gobeil L, Xiong WT, et al. Alternative to body surface area as a solution to correct systematic bias in pediatric echocardiography z scores. *Can J Cardiol*. 2021;37:1790−1797.

26. Nesser HJ, Tkalec W, Patel AR, et al. Quantitation of right ventricular volumes and ejection fraction by three-dimensional echocardiography in patients: comparison with magnetic resonance imaging and radionuclide ventriculography. *Echocardiography*. 2006;23:666−680.

27. Dragulescu A, Grosse-Wortmann L, Fackoury C, Mertens L. Echocardiographic assessment of right ventricular volumes: a comparison of different techniques in children after surgical repair of tetralogy of Fallot. *Eur Heart J Cardiovasc Imaging*. 2012;13:596−604.

28. Koestenberger M, Friedberg MK, Nestaas E, Michel-Behnke I, Hansmann G. Transthoracic echocardiography in the evaluation of pediatric pulmonary hypertension and ventricular dysfunction. *Pulm Circ*. 2016;6:15−29.

29. Renella P, Marx GR, Zhou J, Gauvreau K, Geva T. Feasibility and reproducibility of three-dimensional echocardiographic assessment of right ventricular size and function in pediatric patients. *J Am Soc Echocardiogr*. 2014;27:903−910.

30. Shimada YJ, Shiota M, Sigel RJ, Shiota T. Accuracy of right ventricular volumes and function determined by three-dimensional echocardiography in comparison with magnetic resonance imaging: a meta-analysis study. *J Am Soc Echocardiogr*. 2010;23:943−953.

31. Valente AM, Cook S, Festa P, et al. Multimodality imaging guidelines for patients with repaired tetralogy of Fallot: a report from the American Society of Echocardiography: developed in collaboration with the Society for Cardiovascular Magnetic Resonance and the Society for Pediatric Radiology. *J Am Soc Echocardiogr*. 2014;27:111−141.

32. Gupta S, Khan F, Shapiro M, et al. The associations between tricuspid annular plane systolic excursion (TAPSE), ventricular dyssynchrony, and ventricular interaction in heart failure patients. *Eur J Echocardiogr*. 2008;9:766−771.

33. Fernandez-Friera L, Garcia-Avlarez A, Guzman G, et al. Apical right ventricular dysfunction in patients with pulmonary hypertension demonstrated with magnetic resonance. *Heart*. 2011;97:1250−1256.

34. Shelburne NJ, Parikh KS, Chiswell K, et al. Echocardiographic assessment of right ventricular function and response to therapy in pulmonary arterial hypertension. *Am J Cardiol*. 2019;15:1298−1304.

35. Koestenberger M, Ravekes W, Everett AD, et al. Right ventricular function in infants, children and adolescents: reference values of the tricuspid annular plane systolic excursion (TAPSE) in 640 healthy patients and calculation of z score values. *J Am Soc Echocardiogr*. 2009;22:715−719.

36. Nunez-Gil I, Rubio MD, Carton AJ, et al. Determination of normalized values of the tricuspid annular plane systolic excursion (TAPSE) in 405 Spanish children and adolescents. *Rev Esp Cardiol*. 2011;64:674−680.

37. Madry W, Karolczak MA, Myszkowski M. Critical appraisal of MAPSE and TAPSE usefulness in the postoperative assessment of ventricular contractile function after congenital heart defect surgery in infants. *J Ultrason*. 2019;19:9−16.

38. Mercer-Rosa L, Parnell A, Forfia PR, et al. Tricuspid annular plane systolic excursion in the assessment of right ventricular function in children and adolescents after repair of tetralogy of Fallot. *J Am Soc Echocardiogr*. 2013;26:1322−1329.

39. Hauck A, Guo R, Ivy DD, Younoszai A. Tricuspid annular plane systolic excursion is preserved in young patients with pulmonary hypertension except when associated with repaired congenital heart disease. *Circulation*. 2017;18:1459−1466.

40. Roberson DA, Cui W, Chen Z, Madronero LF, Cuneo BF. Annular and septal Doppler tissue imaging in children: normal z-score tables and effects of age, heart rate, and body surface area. *J Am Soc Echocardiogr*. 2007;20:1276−1284.

41. Cui W, Roberson DA, Chen Z, Madronero LF, Cuneo BF. Systolic and diastolic time intervals measured from Doppler tissue imaging: normal values and Z-score tables, and effects of age, heart rate, and body surface area. *J Am Soc Echocardiogr*. 2008;21:361−370.

42. Lu KJ, Chen JX, Profitis K, et al. Right ventricular global longitudinal strain is an independent predictor of right ventricular function: a multimodality study of cardiac magnetic resonance imaging, real time three-dimensional echocardiography and speckle tracking echocardiography. *Echocardiography*. 2015;32:966−974.

43. Driessen MMP, Hui W, Bijnens BH, et al. Adverse ventricular−ventricular interactions in right ventricular pressure load: insights from pediatric pulmonary hypertension versus pulmonary stenosis. *Physiol Rep*. 2016;4:212833.

44. Kukulski T, Voigt JU, Wilkenshoff UM. A comparison of regional myocardial velocity information derived by pulsed and color Doppler techniques: an in vitro and in vivo study. *Echocardiography*. 2000;17:639−651.

45. Eidem BW, McMahon CJ, Cohen RR, et al. Impact of cardiac growth on Doppler tissue imaging velocities: a study in healthy children. *J Am Soc Echocardiogr*. 2004;17:212−221.

46. Dragulescu A, Grosse-Wortmann L, Redington A, Friedberg MK, Mertens L. Differential effect of right ventricular dilatation on myocardial deformation in patients with atrial septal defects and patients after tetralogy of Fallot repair. *Int J Cardiol*. 2013;168:803−810.

47. Roberson DA, Cui W. Right ventricular Tei index in children: effect of method, age, body surface area, and heart rate. *J Am Soc Echocardiogr*. 2007;20:764−770.

48. Salehian O, Schwerzmann M, Merchant N, et al. Assessment of systemic right ventricular function in patients with transposition of the great arteries using the myocardial performance index: comparison with cardiac magnetic resonance imaging. *Circulation*. 2004;110:3229−3233.

49. Dyer KL, Pauliks LB, Das B, et al. Use of myocardial performance index in pediatric patients with idiopathic pulmonary arterial hypertension. *J Am Soc Echocardiogr*. 2006;19:21−27.

50. Cannesson M, Jacques D, Pinsky MR, Gorcsan J. Effects of modulation of left ventricular contractile state and loading conditions on tissue Doppler myocardial performance index. *Am J Physiol Heart Circ Physiol*. 2006;290:H1952−H1959.

51. Wright L, Negishi K, Dwyer N, Wahi S, Marwick TH. Afterload dependence of right ventricular myocardial strain. J Am Soc Echocardiogr 207;30:676-684.

52. Eyskens B, Ganame J, Claus P, et al. Ultrasonic strain rate and strain imaging of the right ventricle in children before and after percutaneous closure of an atrial septal defect. *J Am Soc Echocardiogr*. 2006;19:994−1000.

53. Jamal F, Bergerot C, Argaud L, Loufouat J, Ovize M. Longitudinal strain quantitates regional right ventricular contractile function. *Am J Physiol Heart Circ Physiol*. 2003;285:H2842−H2847.

54. Badano LP, Kolias TJ, Muraru D, et al. Standardization of left atrial, right ventricular, and right atrial deformation imaging using two-dimensional speckle tracking echocardiography: a consensus document of the EACVI/ASE/Industry Task Force to standardize deformation imaging. *Eur Heart J Cardiovasc Imaging*. 2018;19:591−600.

55. Park J, Choi J, Park SW, et al. Normal references of right ventricular strain values by two-dimensional strain echocardiography according to the age and gender. *Int J Cardiovasc Imaging*. 2018;34:177−183.

56. Hosseinsabet A, Mahmoudian R, Jalali A, Mohseni-Badalabadi R, Davarpasand T. Normal ranges of right atrial strain and strain rate by two-dimensional speckle-tracking echocardiography: a systematic review and meta-analysis. *Front Cardovasc Med*. 2021;8:771647.

57. Muraru D, Haugaa K, Donal E, et al. Right ventricular longitudinal strain in the clinical routine: a state-of-the-art review. *Eur Heart J Cardiovasc Imaging*. 2022;11:jeac022.

58. Menting ME, van den Bosch AE, McGhie JS, et al. Assessment of ventricular function in adults with repaired Tetralogy of Fallot using myocardial deformation imaging. *Eur Heart J Cardiovasc Imaging*. 2015;16:1347−1357.

59. Chow P, Liang X, Cheung EWY, Lam WWM, Cheung Y. New two-dimensional global longitudinal strain and strain rate imaging for assessment of systemic right ventricular function. *Heart*. 2008;94:855−859.

60. Kjaergaard J, Hastrup Svendsen J, Sogaard P, et al. Advanced quantitative echocardiography in arrhythmogenic right ventricular cardiomyopathy. *J Am Soc Echocardiogr*. 2007;20:27−35.

61. Dahou A, Clavel MA, Capoulade R, et al. Right ventricular longitudinal strain for risk stratification in low-flow, low-gradient aortic stenosis with low ejection fraction. *Heart*. 2016;102:548−554.

62. Cantinotti M, Scalese M, Giodano R, et al. Normative data for left and right ventricular systolic strain in healthy Caucasian Italian children by two-dimensional speckle-tracking echocardiography. *J Am Soc Echocardiogr*. 2018;31:712−720.

63. Hulshof HG, Eijsvogels TMS, Kleinnibbelink G, et al. Prognostic value of right ventricular longitudinal strain in patients with pulmonary hypertension: a systematic review and meta-analysis. *Eur Heart J Cardiovasc Imaging*. 2019;32:475−484.

64. Medvedofsky D, Lang RM, Weinert L, et al. 3D echocardiographic global longitudinal strain can identify patients with mildly-to-moderately reduced ejection fraction at higher cardiovascular risk. *Int J Cardiovasc Imaging*. 2019;35:1573−1579.

65. Chahal NS, Lim TK, Jain P, et al. Population-based reference values for 3D echocardiographic LV volumes and ejection fraction. *JACC Cardiovasc Imaging*. 2012;5:1191−1197.

66. Otani K, Babeshima Y, Kitano T, Takeuchi M. Accuracy of fully automated right ventricular quantification software with 3D echocardiography: direct comparison with cardiac magnetic resonance and semi-automated quantification software. *Eur Heart J Cardiovasc Imaging*. 2020;21:787−795.

67. Moceri P, Duchateau N, Baudouy D, et al. Three-dimensional right-ventricular regional deformation and survival in pulmonary hypertension. *Eur Heart J Cardiovasc Imaging*. 2018;19:450−458.

68. Surkova E, Muraru D, Genovese D, et al. Relative prognostic importance of left and right ventricular ejection fraction in patients with cardiac diseases. *J Am Soc Echocardiogr*. 2019;32:1407−1415.

69. Nagata Y, Wu VC, Kado Y, et al. Prognostic value of right ventricular ejection fraction assessed by transthoracic 3D echocardiography. *Circ Cardiovasc Imaging*. 2017;10:e005384.

70. Jone PN, Schafer M, Pan Z, Bremen C, Ivy DD. 3D echocardiographic evaluation of right ventricular function and strain: a prognostic study in paediatric pulmonary hypertension. *Eur Heart J Cardiovasc Imaging*. 2018;19:1026−1033.

71. Jone PN, Duchateau N, Pan Z, Ivy DD, Moceri P. Right ventricular area strain from 3-dimensional echocardiography: mechanistic insight of right ventricular dysfunction in pediatric pulmonary hypertension. *J Heart Lung Transplant*. 2021;40:138−148.

72. Sano S, Fujii Y, Kasahara S, et al. Repair of Ebstein's anomaly in neonates and small infants: impact of right ventricular exclusion and its indications. *Eur J Cardiothorac Surg*. 2014;45:549−555.

73. Mizuno M, Hoashi T, Sakaguchi H, et al. Application of cone reconstruction for neonatal Ebstein anomaly or tricuspid valve dysplasia. *Ann Thorac Surg*. 2016;101:1811−1817.

74. Mawad W, Friedberg MK. The continuing challenge of evaluating diastolic function by echocardiography in children: developing concepts and newer modalities. *Curr Opin Cardiol*. 2017;32:93−100.

75. Hodzic A, Bobin P, Mika D, et al. Standard and strain measurements by echocardiography detect early overloaded right ventricular dysfunction: validation against hemodynamic and myocyte contractility changes in a large animal model. *J Am Soc Echocardiogr*. 2017;30:1138−1147.

76. Zoghbi WA, Habib GB, Quinones MA. Doppler assessment of right ventricular filling in a normal population. Comparison with left ventricular filling dynamics. *Circulation*. 1990;82:1316−1324.

77. Heywood JT, Grimm J, Hess OM, Jakob M, Krayenbuhl HP. Right ventricular diastolic function during exercise: effect of ischemia. *J Am Coll Cardiol*. 1990;16:611−622.

78. Nagueh SF, Kopelen HA, Zoghbi WA. Relation of mean right atrial pressure to echocardiographic and Doppler parameters of right atrial and right ventricular function. *Circulation*. 1996;93:1160−1169.

79. Mah K, Bruce A, Zahari N, et al. Tilt-table echocardiography unmasks early diastolic dysfunction in patients with hemoglobinopathies. *J Pediatr Hematol Oncol*. 2020;42:391−397.

80. Jhaveri S, Komarlu R, Worley S, et al. Left atrial strain and function in pediatric hypertrophic cardiomyopathy. *J Am Soc Echocardiogr*. 2021;34:996−1006.

81. Loar RW, Pignatelli RH, Morris SA, et al. Left atrial strain correlates with elevated filling pressures in pediatric heart transplantation recipients. *J Am Soc Echocardiogr*. 2020;33:504−511.

82. Vakilian F, Tavallaie A, Alimi H, Poorzand H, Salehi M. Right atrial strain in the assessment of right heart mechanics in patients with heart failure with reduced ejection fraction. *J Cardiovasc Imaging*. 2021;29:135−143.

83. Hasselberg N, Kagiyama N, Soyama Y, et al. The prognostic value of right atrial strain imaging in patients with precapillary pulmonary hypertension. *J Am Soc Echocardiogr*. 2021;34:851−861.

84. Jone PN, Schafer M, Li L, et al. Right atrial deformation in predicting outcomes in pediatric pulmonary hypertension. *Circ Cardiovasc Imaging*. 2017;10:e006250.

85. Mertens L. Right atrial contractile function in pediatric pulmonary hypertension: a novel marker for disease severity? *Circ Cardiovasc Imaging*. 2017;10:e007264.

86. Van den Eynde J, Derdeyn E, Schuermans A, et al. End-diastolic forward flow and restrictive physiology in repaired tetralogy of Fallot: a systematic review and meta-analysis. *J Am Heart Assoc*. 2022;11:e024036.

87. Redington AN, Penny D, Rigby ML. Antegrade diastolic pulmonary artery flow as a marker of right ventricular restriction after complete repair of pulmonary atresia with intact ventricular septum and critical pulmonary valve stenosis. *Cardiol Young*. 1992;2:382−386.

88. Ahmad N, Kantor PF, Grosse-Wortmann L, et al. Influence of RV restrictive physiology on LV diastolic function in children after tetralogy of Fallot repair. *J Am Soc Echocardiogr*. 2012;25:866−873.

89. Nogard G, Gatzoulis MA, Josen M, Cullen S, Redington AN. Does restrictive right ventricular physiology in the early postoperative period predict subsequent right ventricular restriction after repair of tetralogy of Fallot? *Heart*. 1998;79:481−484.

90. Schmitz L, Stiller B, Pees C, et al. Doppler-derived parameters of diastolic left ventricular function in preterm infants with a birth weight <1500 g: reference values and differences to term infants. *Early Hum Dev*. 2004;76:101−114.

91. Spinner EM, Shannon P, Buice D, et al. In vitro characterization of the mechanisms responsible for functional tricuspid regurgitation. *Circulation*. 2011;124:920−929.

92. Stankovic I, Daraban AM, Jasaityte R, et al. Incremental value of the en face view of the tricuspid valve by two-dimensional and three-dimensional echocardiography for accurate identification of tricuspid valve leaflets. *J Am Soc Echocardiogr*. 2014;27:376−384.

93. Mah K, Khoo NS, Martin B, et al. Insights from 3D echocardiography in hypoplastic left heart syndrome patients undergoing TV repair. *Pediatr Cardiol*. 2022;43:735−743.

94. Mah K, Khoo NS, Tham E, et al. Tricuspid regurgitation in hypoplastic left heart syndrome: three-dimensional echocardiography provides additional information in describing jet location. *J Am Soc Echocardiogr*. 2021;34:529−536.

95. Shigemitsu S, Mah K, Thompson RB, et al. Tricuspid valve tethering is associated with residual regurgitation after valve repair in hypoplastic left heart syndrome: a three-dimensional echocardiography study. *J Am Soc Echocardiogr*. 2021;11:1199−1210.

96. Simpson J, Lopez L, Acar P, Friedberg MK, et al. Three-dimensional echocardiography in congenital heart disease: an expert consensus document from the European Association of Cardiovascular Imaging and the American Society of Echocardiography. *J Am Soc Echocardiogr*. 2016;17:1071−1097.

97. Hauser M, Bengel FM, Hager A, et al. Impaired myocardial blood flow and coronary flow reserve of the anatomical right systemic ventricle in patients with congenitally corrected transposition of the great arteries. *Heart*. 2003;89:1231−1235.

98. Moceri P, Bouvier P, Baudouy D, et al. Cardiac remodelling amongst adults with various aetiologies of pulmonary arterial hypertension including Eisenmenger syndrome—implications on survival and the role of right ventricular transverse strain. *Eur Heart J Cardiovasc Imaging*. 2017;18:1262−1270.

99. Galiè N, Hoeper MM, Humbert M, et al. Guidelines for the diagnosis and treatment of pulmonary hypertension: the Task Force for the Diagnosis and Treatment of Pulmonary Hypertension of the European Society of Cardiology (ESC) and the European Respiratory Society (ERS), endorsed by the International Society of Heart and Lung Transplantation (ISHLT). *Eur Heart J*. 2009;30:2493−2537.

100. Lindner JR, Mathier MA, McGoon MD, et al. ACCF/AHA 2009 expert consensus document on pulmonary hypertension a report of the American College of Cardiology Foundation Task Force on Expert Consensus Documents and the American Heart Association developed in collaboration with the American College of Chest Physicians; American Thoracic Society, Inc.; and the Pulmonary Hypertension Association. *J Am Coll Cardiol*. 2009;53:1573−1619.

101. Raymond RJ, Hinderliter AL, Willis PW, et al. Echocardiographic predictors of adverse outcomes in primary pulmonary hypertension. *J Am Coll Cardiol*. 2002;39:1214−1219.

102. Siddiqui I, Rajagopal S, Brucker A, et al. Clinical and echocardiographic predictors of outcomes in patients with pulmonary hypertension. *Am J Cardiol*. 2018;122:872−878.

103. Grapsa J, Hunes MCP, Tan TC, et al. Echocardiographic and hemodynamic predictors of survival in precapillary pulmonary hypertension. *Circ Cardiovasc Imaging*. 2015;8:e002107.

104. Alenezi F, Mandawat A, ll'Giovine ZJ, et al. Clinical utility and prognostic value of right atrial function in pulmonary hypertension. *Circ Cardiovasc Imaging*. 2018;11:e006984.

105. Jone PN, Ivy DD. Echocardiography in pediatric pulmonary hypertension. *Front Pediatr*. 2014;2:124.

106. Driessen MMP, Leiner T, Siesward GTJ, et al. RV adaptation to increased afterload in congenital heart disease and pulmonary hypertension. *PLoS One*. 2018;13:e0205196.

107. Lam YY, Kaya MG, Gotekin O, Gatzoulis MA, Li W, Henein MY. Restrictive right ventricular physiology: its presence and symptomatic contribution in patients with pulmonary valvular stenosis. *J Am Coll Cardiol*. 2007;50:1491−1497.

108. Pettersen E, Helle-Valle T, Edvardsen T, et al. Contraction pattern of the systemic right ventricle shift from longitudinal to circumferential shortening and absent global ventricular torsion. *J Am Coll Cardiol*. 2007;49:2450−2456.

109. Kollars CAK, Gelehrter S, Bove EL, Ensing G. Effects of morphologic left ventricular pressure on right ventricular geometry and tricuspid valve regurgitation in patients with congenitally corrected transposition of the great arteries. *Am J Cardiol*. 2010;105:735−739.

110. Miranda WR, Jain CC, Connolly HM, et al. Prevalence of pulmonary hypertension in adults after atrial switch and role of ventricular filling pressures. *Heart*. 2021;107:468−473.

111. Chaix MA, Dore A, Mercier LA, et al. Late onset postcapillary pulmonary hypertension in patients with transposition of the great arteries and Mustard or Senning baffles. *J Am Heart Assoc*. 2017;6:e006481.

112. Khoo NS, Smallhorn JF, Kaneko S, Myers K, Kutty S, Tham EB. Novel insights into RV adaptation and function in hypoplastic left heart syndrome between the first 2 stages of surgical palliation. *J Am Coll Cardiol Img*. 2011;4:128−137.

113. Khoo NS, Smallhorn JF, Kaneko S, Kutty S, Altamirano L, Tham EB. The assessment of atrial function in single ventricle hearts from birth to Fontan: a speckle-tracking study by using strain and strain rate. *J Am Soc Echocardiogr*. 2013;26:756−764.

114. Rosner A, Bharucha T, James A, Mertens L, Friedberg MK. Impact of right ventricular geometry and left ventricular hypertrophy on right ventricular mechanics and clinical outcomes in hypoplastic left heart syndrome. *J Am Soc Echocardiogr*. 2019;32:1350−1358.

115. Rana BS, Robinson S, Francis R, et al. Tricuspid regurgitation and the right ventricle in risk stratification and timing of intervention. *Echo Res Pract*. 2019;6:R25−R39.

116. Barber G, Helton JG, Aglira BA, et al. The significance of tricuspid regurgitation in hypoplastic left-heart syndrome. *Am Heart J*. 1988;116:1563.

117. Colquitt JL, Loar RW, Morris SA, Feagin DK, Sami S, Pignatelli RH. Serial strain analysis identifies hypoplastic left heart syndrome infants at risk for cardiac morbidity and mortality: a pilot study. *J Am Soc Echocardiogr*. 2019;32:643−650.

118. Kutty S, Colen T, Thompson RB, et al. Tricuspid regurgitation in hypoplastic left heart syndrome: mechanistic insights from 3-dimensional echocardiography and relationship with outcomes. *Circ Cardiovasc Imaging*. 2014;7:765−772.

119. Colen T, Kutty S, Thompson RB, et al. Tricuspid valve adaptation during the first interstage period in hypoplastic left heart syndrome. *J Am Soc Echocardiogr*. 2018;31:624−633.

120. Xu Q, Sun L, Zhou W, et al. Evaluation of right ventricular myocardial strains by speckle tracking echocardiography after percutaneous device closure of atrial septal defects in children. *Echocardiography*. 2018;35:1183−1188.

121. Van de Bruaene A, Buys R, Vanhees L, Delcroix M, Voigt J, Budts W. Regional right ventricular deformation in patients with open and closed atrial septal defect. *Eur J Echocardiogr*. 2011;12:206−213.

122. Umemoto S, Sakamoto I, Abe K, et al. Preoperative threshold for normalizing right ventricular volume after transcatheter closure of adult atrial septal defect. *Circ J*. 2020;84:1312−1319.

123. Pauliks LB, Chan KK, Chang D, et al. Regional myocardial velocities and isovolumic contraction acceleration before and after device closure of atrial septal defects: a color tissue Doppler study. *Am Heart J*. 2005;150:294−301.

124. Miranda WR, Hagler DJ, Reeder GS, et al. Temporary balloon occlusion of atrial septal defects in suspected or documented left ventricular diastolic dysfunction: hemodynamic and clinical findings. *Catheter Cardiovasc Interv*. 2019;93:1069−1075.

125. Shin YR, Jung JW, Kim NK, et al. Factors associated with progression of right ventricular enlargement and dysfunction after repair of tetralogy of Fallot based on serial cardiac magnetic resonance imaging. *Eur J Cardiothorac Surg*. 2016;50:464−469.

126. Wald RM, Valente AM, Gauvreau K, et al. Cardiac magnetic resonance markers of progressive RV dilation and dysfunction after tetralogy of Fallot repair. *Heart*. 2015;101:1724−1730.

127. Lee JK, Chikkabyrappa SM, Bhat A, Buddhe S. Echocardiographic assessment of right ventricular volume in repaired tetralogy of Fallot: a novel approach to an older technique. *J Echocardiogr*. 2022;20:106−114.

128. Alghamdi MH, Grosse-Wortmann L, Ahmad N, Mertens L, Friedberg MK. Can simple echocardiographic measures reduce the number of cardiac magnetic resonance imaging studies to diagnose right ventricular enlargement in congenital heart disease? *J Am Soc Echocardiogr*. 2012;25:518−523.

129. D'Anna C, Caputi A, Natali B, et al. Improving the role of echocardiography in studying the right ventricle of repaired tetralogy of Fallot patients: comparison with cardiac magnetic resonance. *Int J Cardiovasc Imaging*. 2018;34:399−406.

130. Li VW, Yu CK, So EK, Wong WH, Cheung Y. Ventricular myocardial deformation imaging of patients with repaired tetralogy of Fallot. *J Am Soc Echocardiogr*. 2020;33:788−801.

131. Koestenberger M, Nagel B, Ravekes W, et al. Systolic right ventricular function in pediatric and adolescent patients with tetralogy of Fallot: echocardiography versus magnetic resonance imaging. *J Am Soc Echocardiogr*. 2011;24:45−52.

132. Dragulescu A, Friedberg MK. A tale of two ventricles: ventricular−ventricular interactions and LV dysfunction after surgical repair of tetralogy of Fallot. *Eur Heart J Cardiovasc Imaging*. 2014;15:498−499.

133. Bokma JP, Winter MM, Oosterhof T, et al. Severe tricuspid regurgitation is predictive for adverse events in tetralogy of Fallot. *Heart*. 2015;101:794−799.

134. Badiu CC, Schreiber C, Horer J, et al. Early timing of surgical intervention in patients with Ebstein's anomaly predicts superior long-term outcome. *Eur J Cardiothoracic Surg*. 2010;37:186−192.

135. Perdreau E, Tsang V, Hughes ML, et al. Change in biventricular function after cone reconstruction of Ebstein's anomaly: an echocardiographic study. *Eur Heart J Cardiovasc Imaging*. 2018;19:808−815.

136. Lu X, Nadvoretskiy V, Bu L, et al. Accuracy and reproducibility of real-time three-dimensional echocardiography for assessment of right ventricular volumes and ejection fraction in children. *J Am Soc Echocardiogr*. 2008;21:84−89.

137. Celermajer DS, Bull C, Till JA, et al. Ebstein's anomaly: presentation and outcome from fetus to adult. *J Am Coll Cardiol*. 1994;23:170−176.

138. Tobler D, Yalonetsky S, Crean AM, et al. Right heart characteristics and exercise parameters in adults with Ebstein anomaly: new perspectives from cardiac magnetic resonance imaging studies. *Int J Cardiol*. 2013;165:146−150.

139. Kuhn A, Meierhofer C, Rutz T, et al. Non-volumetric echocardiographic indices and qualitative assessment of right ventricular systolic function in Ebstein's anomaly: comparison with CMR-derived ejection fraction in 49 patients. *Eur Heart J Cardiovasc Imaging*. 2016;17:930−935.

140. Valsangiacomo Buechel ER, Mertens LL. Imaging the right heart: the use of multi-modality imaging. *Eur Heart J*. 2012;33:940−960.

141. Oechslin E, Buchholz S, Jenni R. Ebstein's anomaly in adults: Doppler-echocardiographic evaluation. *Thorac Cardiovasc Surg*. 2000;48:209−213.

142. Eckersley LG, Howley LW, van der Velde ME, et al. Quantitative assessment of left ventricular dysfunction in fetal Ebstein's anomaly and tricuspid valve dysplasia. *J Am Soc Echocardiogr*. 2019;32:1598−1607.

143. Lianza AC, Rodrigues ACT, Mercer-Rosa L, et al. Right ventricular systolic function after the cone procedure for Ebstein's anomaly: comparison between echocardiography and cardiac magnetic resonance. *Pediatr Cardiol*. 2020;41:985−995.

144. Edwards WD. Embryology and pathologic features of Ebstein's anomaly. *Prog Pediatr Cardiol*. 1993;2:5−15.

145. Shiina A, Seward JB, Edwards WD, Hagler DJ, Tajik AJ. Two-dimensional echocardiographic spectrum of Ebstein's anomaly: detailed anatomic assessment. *J Am Coll Cardiol*. 1984;3:356−370.

146. Paranon S, Acar P. Ebstein's anomaly of the tricuspid valve: from fetus to adult: congenital heart disease. *Heart*. 2008;94:237−243.

147. Roberson DA, Silverman NH. Ebstein's anomaly: echocardiographic and clinical features in the fetus and neonate. *J Am Coll Cardiol*. 1989;14:1300−1307.

148. Patel V, Nanda NC, Rajdev S, et al. Live/real time three-dimensional transthoracic echocardiographic assessment of Ebstein's anomaly. *Echocardiography*. 2005;22:847−854.

149. Velayudhan DE, Brown TM, Nanda NC, et al. Quantification of tricuspid regurgitation by live three dimensional transthoracic

echocardiographic measurements of vena contracta area. *Echocardiography*. 2006;23:793–800.

150. Ahmed S, Nanda NC, Nekkanti R, Pacifico AD. Transesophageal three-dimensional echocardiographic demonstration of Ebstein's anomaly. *Echocardiography*. 2003;20:305–307.

151. Vettukattil JJ, Bharucha T, Anderson RH. Defining Ebstein's malformation using three-dimensional echocardiography. *Interactive Cardiovasc Thorac Surg*. 2007;6:685–690.

152. Levy PT, Sanchez A, Machefsky A, Fowler S, Holland M, Singh GK. Normal ranges of right ventricular systolic and diastolic strain measures in children: a systematic review and meta-analysis. *J Am Soc Echocardiogr*. 2014;27:549–560.

153. Uysal F, Nostan OM. Determination of reference values for tricuspid annular plane systolic excursion in healthy Turkish children. *Anatol J Cardiol*. 2016;16:354–359.

154. Johnson GL, Moffett CB, Noonan JA. Doppler echocardiographic studies of diastolic ventricular filling patterns in premature infants. *Am Heart J*. 1988;116:1568–1573.

155. Ciccone MM, Scicchitano P, Zito A, et al. Different functional cardiac characteristics observed in term/preterm neonates by echocardiography and tissue Doppler imaging. *Early Hum Dev*. 2011;87:555–558.

156. Vorhies E, Gajarski RJ, Yu S, Donohue JE, Fifer CG. Echocardiographic evaluation of ventricular function in children with pulmonary hypertension. *Pediatr Cardiol*. 2014;35:759–766.

157. Rafeiyian S, Looti-Shahrokh B, Motamedi M, Karkhaneh-Yousefi Z, Mojtahedzadeh S, Kouhi A. Pulse tissue Doppler analysis of tricuspid annular motion in Iranian children. *Int J Cardiovasc Imaging*. 2006;22:363–367.

158. Swaminathan S, Ferrer P, Wolff G, Gomez-Marin O, Rusconi PG. Usefulness of tissue Doppler echocardiography for evaluating ventricular function in children without heart disease. *Am J Cardiol*. 2003;91:570–574.

159. GronerA, Yau J, Lytrivi ID, et al. The role of right ventricular function in paediatric idiopathic dilated cardiomyopathy. *Cardiol Young*. 2013;23:409–415.

160. Jone PN, Hinzman J, Wagner BD, Ivy DD, Younoszai A. Right ventricular to left ventricular diameter ratio at end systole in evaluating outcomes in children with pulmonary hypertension. *J Am Soc Echocardiogr*. 2014;27:172–178.